HuH-7, and cervical carcinoma HeLa–and subjected them to the cell cycle analysis described above. The results revealed that S phase progression was delayed in NKNT-3, but not in HuH-7 or HeLa cells (Fig. 2B). This indicates that the delay of the cell cycle by NS5B expression is not limited to PH5CH8 cells.

IFN-β mediates the delay of S phase progression by NS5B

Since it has been reported previously that IFN-β induced the delay of S phase progression in human cultured cells (Vannucchi et al., 2000), we speculated that IFN-β was

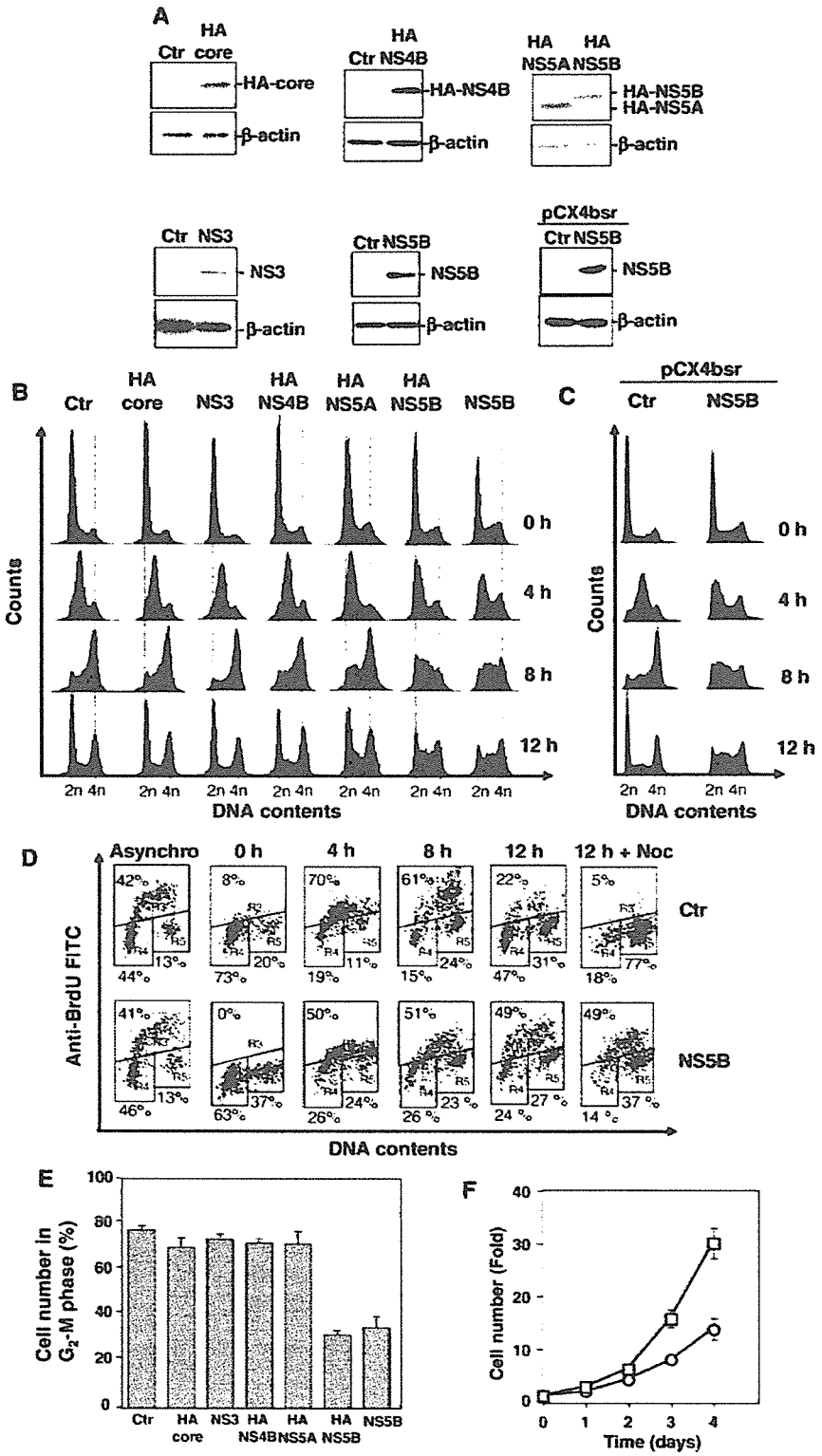

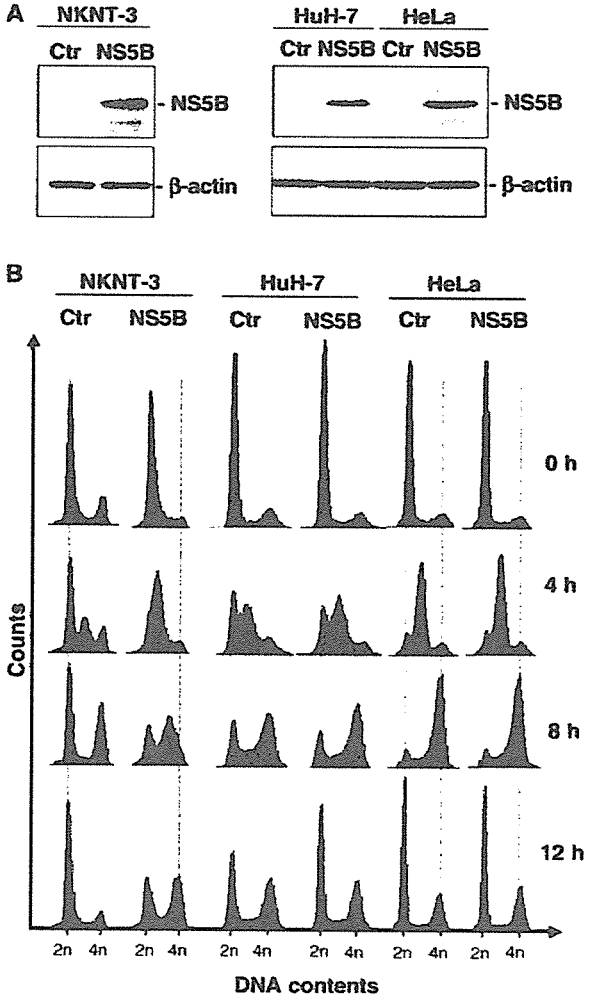

Fig. 2. NS5B delays S phase progression in another immortalized human hepatocytes. (A) Western blot analysis of NKNT-3, HuH-7, and HeLa cells infected with pCXbsr retrovirus encoding NS5B. The pCXbsr retrovirus was used as a control infection (Ctr). Anti-NS5B and anti-β-actin antibodies were used for the immunoblotting analysis. (B) Cell cycle analysis of NKNT-3, HuH-7, and HeLa cells expressing NS5B. NKNT-3, HuH-7, and HeLa cells that expressed NS5B (NS5B series) were synchronized, and cell cycle progression was analyzed as indicated in Fig. 1B. NKNT-3, HuH-7, and HeLa cells that were infected with the pCXbsr retrovirus were also analyzed as a control (Ctr series).

induced by NS5B. To evaluate this hypothesis, we examined whether or not PH/NS5B and NKNT-3 cells expressing NS5B (NK/NS5B) induce the expression of IFN-β. RT-PCR analysis clearly indicated that they did, and, at the same time, we found that HuH-7 and HeLa cells did not, despite their expression of NS5B (Fig. 3A). We next examined whether or not S phase progression is delayed in PH5CH8 and NKNT-3 cells treated with IFN-β prior to release from the G1/S boundary. As we expected, the S phase progression was stalled in PH5CH8 and NKNT-3 cells treated with IFN-β (Fig. 3B). We also observed that IFN-γ did not possess this activity of IFN-β (data not shown). These results suggest that the induction of IFN-β is implicated in the cell cycle delay in two immortalized human hepatocyte cell lines, PH5CH8 and NKNT-3.

To confirm the effect of IFN-β on cell cycle delay, we further examined whether or not treatment with anti-IFN-β neutralizing antibody can restore the cell cycle delay in PH/NS5B cells. The results showed that this treatment canceled the delay of S phase progression in PH/NS5B cells (Fig. 4A). BrdUrd incorporation analysis also showed that the proportion of cells reaching the G2-M phase was increased by the treatment with anti-IFN-β antibody in PH/NS5B cells (Fig 4B). These observations indicated that the expression of IFN-β mediated cell cycle delay during the S phase in PH/NS5B cells and suggested that the expression of NS5B induced IFN-β in PH5CH8 and NKNT-3 cells even without replication of the viral genome.

Activation of TLR3 signaling pathway by NS5B

Since IFN-β is known as a major cytokine induced by the activation of the TLR3 and TLR4 signaling pathways (Takeda et al., 2003), we next focused on which TLR pathway was activated for the production of IFN-β in PH/NS5B cells. To answer this question, TLR3- and TLR4-specific siRNAs were used to knock down TLR3 and TLR4 expression in PH/NS5B cells. TLR3 and TLR4 mRNAs were drastically decreased in PH/NS5B cells transfected with TLR3 and TLR4 siRNAs, respectively, but not in PH/NS5B cells transfected with GL2 siRNA (Elbashir et al., 2001) used as a control (Fig. 5A). This result indicates that the siRNAs used specifically contribute well to the degradation of TLR3 and TLR4 mRNAs. In this condition, IFN-β mRNA was significantly decreased in only PH/NS5B cells transfected with TLR3 siRNA (Fig. 5A), indicating that IFN-β expression in PH/NS5B cells is mediated through the TLR3 signaling pathway. The growth rate of PH/NS5B cells transfected with TLR3 siRNA was also accelerated, although TLR4 siRNA showed a rather lethal effect (Fig. 5B).

Fig. 1. HCV NS5B causes the delay of S phase progression. (A) Expression of HCV proteins in human cells introduced by retrovirus-mediated gene transfer. Western blot analysis of PH5CH8 cells infected with pCXbsr retroviruses encoding HCV proteins (HA-core, NS3, HA-NS4B, HA-NS5A, HA-NS5B, and NS5B) or pCX4bsr retrovirus encoding NS5B. pCXbsr or pCX4bsr retrovirus was used as a control infection (Ctr). Anti-HA (3F10, Roche), anti-NS3 (Novacastra), anti-NS5B, and anti-β-actin (Sigma) antibodies were used for the immunoblotting analysis. (B) Cell cycle analysis of PH5CH8 cells expressing HCV proteins. PH5CH8 cells that expressed HA-core, NS3, HA-NS4B, HA-NS5A, HA-NS5B, or NS5B were synchronized at G1/S boundary, and then cell cycle progression was monitored by flow cytometry after the release of the cells into the S phase at the indicated times. PH/Ctr cells that were infected with pCXbsr retrovirus were also analyzed as a control. (C) Cell cycle analysis of PH5CH8 cells infected with pCX4bsr retrovirus encoding NS5B. The cell cycle analysis was performed as described in panel B. (D) BrdUrd incorporation analysis of PH/Ctr and PH/NS5B cells. Cell cycle distribution of dot-plots of BrdUrd fluorescence versus DNA contents was analyzed in asynchronous or synchronized PH/Ctr and PH/NS5B cells. To measure the cells reaching the G2-M phase at 12 h after release, the cells were accumulated by Noc treatment. (E) Analysis of the cells reaching the G2-M phase. The percentage of cells at that phase was assessed by Noc treatment as indicated in panel D. The data are means ± SD of values from three independent experiments. (F) Growth curve of PH/Ctr and PH/NS5B cells. PH/Ctr (squares) or PH/NS5B (circles) were plated onto 6-well plates (3×10^4 cells per well), and the kinetics of cell proliferation during 4 days in culture were determined by trypan blue treatment. The data indicate average values ± SD from three independent experiments.

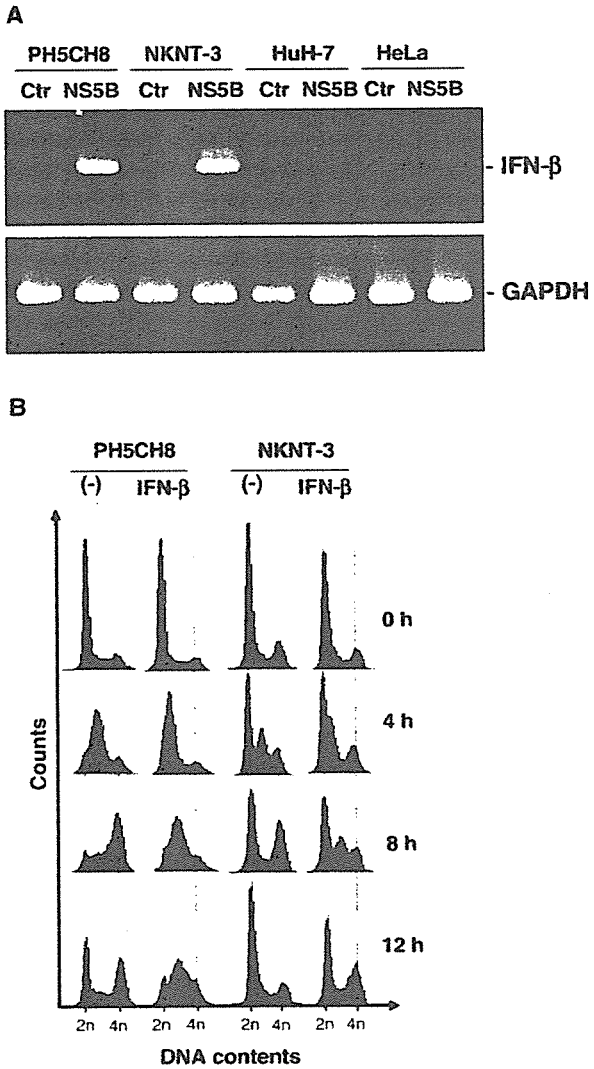

Fig. 3. IFN-β mediates the delay of S phase progression by NS5B. (A) RT-PCR analysis of IFN-β mRNA. The total RNAs were extracted from PH5CH8, NKNT-3, HuH-7, and HeLa cells (Ctr and NS5B series) and were subjected to RT-PCR analysis using primer sets for IFN-β (341 bp) and GAPDH (587 bp). (B) Cell cycle analysis of PH5CH8 and NKNT-3 cells treated with or without IFN-β. PH5CH8 and NKNT-3 cells were treated with or without IFN-β (500 IU/ml) at 12 h prior to release, and cell cycle progression was analyzed as indicated in Fig. 1B.

Furthermore, BrdUrd incorporation analysis using the Noc treatment revealed that 56% of PH/NS5B cells transfected with TLR3 siRNA reached the G2-M phase at 12 h after release, while only 33% of PH/NS5B cells transfected with GL2 siRNA reached that phase (Fig. 5C). The percentage of G2-M phase cells at 12 h after release was also 34% in PH/NS5B cells transfected with TLR4 siRNA, although the growth rate of these cells was lower than that of cells transfected with GL2 siRNA. These results indicated that the induction of IFN-β by NS5B expression was mediated through the activation of the TLR3 signaling pathway. This, in turn, demonstrated that TLR3 siRNA could override the delay of S phase progression in PH/NS5B cells.

To obtain further evidence that the induction of IFN-β by NS5B is mediated through TLR3, we prepared human embryonic kidney (HEK) 293 cells stably expressing TLR3 derived from PH5CH8 cells since it has been reported that ectopic expression of TLR3 can reconstruct the TLR3 signaling pathway in HEK293 cells (Alexopoulou et al., 2001). First, HEK293 cells were infected with retrovirus pCXbsr encoding NS5B or pCXbsr as a negative control (Ctr), yielding HEK293 cells (HEK/NS5B) stably expressing NS5B and control HEK293 cells (HEK/Ctr). Next, HEK/NS5B and HEK/Ctr cells were infected with

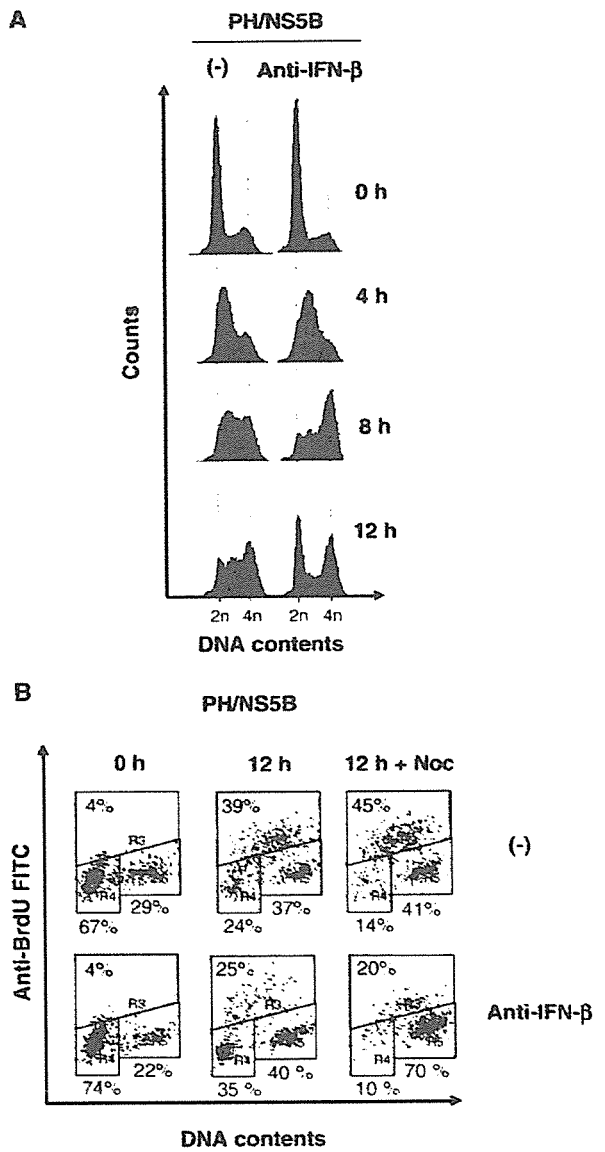

Fig. 4. Treatment with anti-IFN-β antibody canceled the delay of S phase progression. (A) Cell cycle analysis of PH/NS5B cells treated with or without anti-IFN-β antibody. PH/NS5B cells were treated with anti-IFN-β antibody (70 U/ml, Oxford Biotechnology) during cell cycle synchronization and after release from the G1/S boundary. (B) BrdUrd incorporation analysis of PH/NS5B cells treated with or without anti-IFN-β antibody. The antibody was used as indicated in panel A. Noc was used as indicated in Fig. 1D.

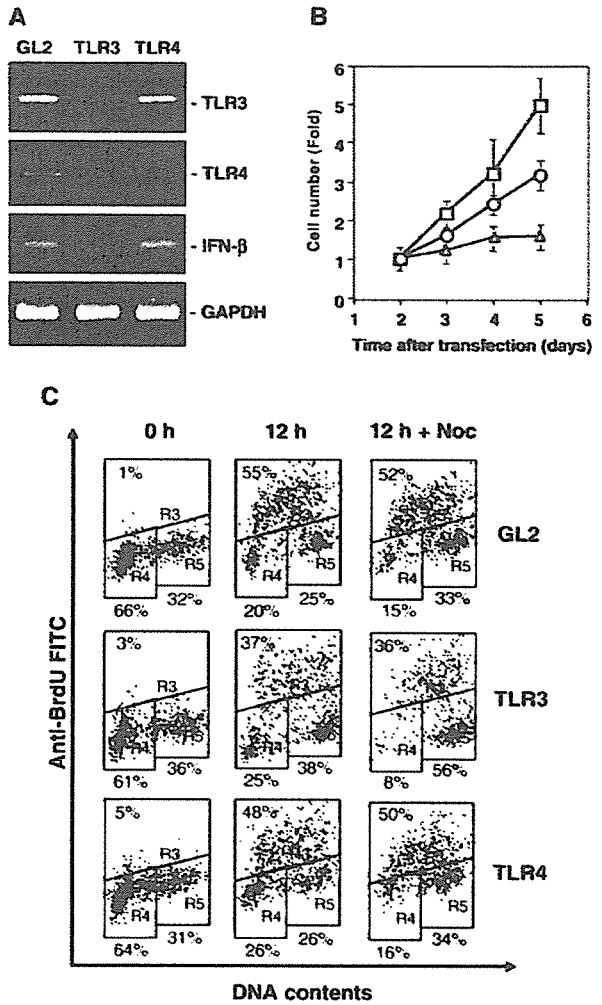

Fig. 5. Activation of IFN-β gene by NS5B is mediated through the TLR3 signaling pathway. (A) Down-regulation of IFN-β mRNA by transfection of TLR3 siRNA. PH/NS5B cells were transfected with dsRNA duplexes targeting TLR3, TLR4, or luciferase GL2. After 3 days, the expression levels of TLR3, TLR4, IFN-β, and GAPDH mRNAs were examined by RT-PCR. (B) Growth curve of PH/NS5B cells transfected with siRNAs. After 2 days of transfection, the proliferation kinetics of PH/NS5B cells transfected with GL2 (circles), TLR3 (squares), and TLR4 (triangles) siRNAs were analyzed as indicated in Fig. 1F. (C) BrdUrd incorporation analysis of PH/NS5B cells transfected with GL2, TLR3, and TLR4 siRNAs. After 2 days of transfection, the cells were synchronized, and cell cycle progression was analyzed as indicated in Fig. 1D.

retrovirus pCXpur encoding TLR3 or pCXpur as a negative control, yielding cells stably expressing TLR3 and control HEK293 cells. The expression of NS5B or TLR3 was confirmed by Western blot analysis (Fig. 6A). We then performed a dual-luciferase reporter assay using an IFN-β gene promoter. The results revealed that the luciferase activity was enhanced in only the HEK293 cells stably expressing both NS5B and TLR3 (Fig. 6B). This suggests that TLR3 mediates NS5B's induction of IFN-β. However, since the enhancement of luciferase activity was approximately two-fold, we failed to detect the enhancement of the mRNA expression levels for IFN-β and one of its target genes, ISG56 (data not shown). To accurately assess the enhancement, high expression levels of NS5B and TLR3 in HEK293 cells will be needed.

The RIG-I-mediated signaling pathway is not implicated in the induction of IFN-β in PH/NS5B cells

Recently, RIG-I, a cellular DExD/H box helicase, was found to be a double-stranded RNA (dsRNA) binding protein that functions independently of TLR3 to induce IFN-β in response to viral infection (Yoneyama et al., 2004). Since another recent study showed that both the TLR3- and RIG-I-mediated signaling pathways are functional in PH5CH8 cells (Li et al., 2005a, 2005b), we examined whether or not the RIG-I-mediated signaling pathway is involved in NS5B's induction of IFN-β. First, PH/NS5B and PH/Ctr cells were infected with retrovirus pCXpur encoding myc-tagged RIG-IC, a dominant negative inhibitor of RIG-I harboring only the helicase domain but not the two N-terminal CARD domains (Yoneyama et al., 2004), or pCXpur as a negative control. Cells that stably expressed myc-tagged RIG-IC were thus obtained. The expression of myc-

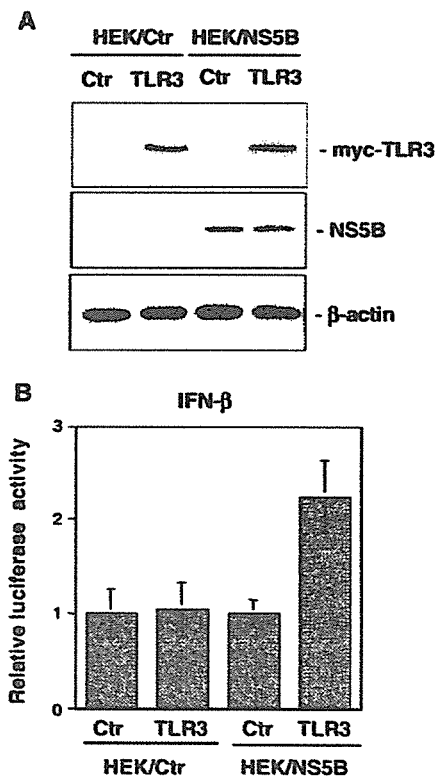

Fig. 6. Ectopic expression of TLR3 enhances the IFN-β gene promoter in only the HEK293 cells stably expressing NS5B. (A) Expression of TLR3 and NS5B in HEK293 cells introduced by retrovirus-mediated gene transfer. Western blot analysis of HEK/Ctr or HEK/NS5B cells infected with pCXpur retrovirus encoding myc-tagged TLR3 was performed. The pCXpur retrovirus was used as a control infection. Anti-myc, anti-NS5B, and anti-β-actin antibodies were used for the immunoblotting analysis. (B) Dual luciferase reporter assay of the IFN-β gene promoter. The cells shown in panel A were transfected with pIFN-β(-125)-Luc, and the dual luciferase assay was performed as described previously (Dansako et al., 2003). Data are means ± SD from three independent triplicate experiments.

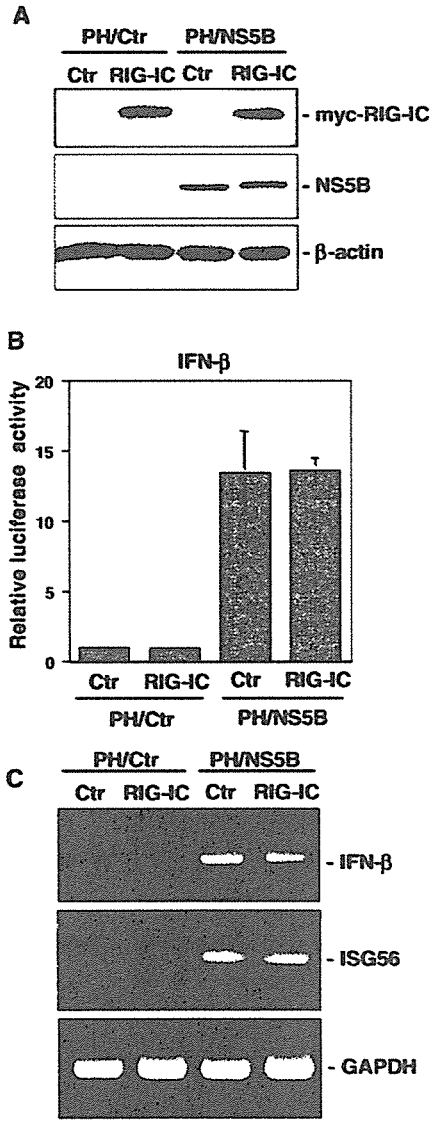

Fig. 7. Induction of IFN-β by NS5B is not mediated through the RIG-I signaling pathway. (A) Expression of RIG-IC and NS5B in PH5CH8 cells introduced by retrovirus-mediated gene transfer. Western blot analysis of PH/Ctr or PH/NS5B cells infected with pCXpur retrovirus encoding myc-tagged RIG-IC was performed. The pCXpur retrovirus was used as a control infection. Anti-myc, anti-NS5B, and anti-β-actin antibodies were used for the immunoblotting analysis. (B) Dual luciferase reporter assay of the IFN-β gene promoter. The cells shown in panel A were transfected with pIFN-β(-125)-Luc, and the dual luciferase assay was performed as indicated in Fig. 6B. (C) RT-PCR analysis of IFN-β and ISG56 mRNAs. The total RNAs were extracted from the cells shown in panel A and subjected to RT-PCR analysis using primer sets for IFN-β (341 bp), ISG56 (320 bp), and GAPDH (587 bp).

tagged RIG-IC was confirmed by Western blot analysis (Fig. 7A). Using PH/Ctr cells stably expressing myc-tagged RIG-IC, we confirmed that IFN-β production was markedly suppressed after infection with Sendai virus (data not shown), as initially observed in Newcastle disease virus infection (Yoneyama et al., 2004). This indicates that RIG-IC functions as a dominant negative inhibitor of RIG-I in PH5CH8 cells. We then performed a dual-luciferase reporter assay using an *IFN-β* gene promoter. The results revealed that the enhancement of luciferase activity in PH/NS5B cells was not suppressed regardless of RIG-IC expression (Fig. 7B). Furthermore, the mRNA expression levels for IFN-β and one of its target genes, ISG56, were also unchanged by the expression of RIG-IC (Fig. 7C). These results suggest that NS5B's induction of IFN-β is not mediated through the RIG-I signaling pathway.

NS5B does not interact with TLR3 adaptor protein

Since we showed that NS5B's induction of IFN-β was mediated through the TLR3 but not the RIG-I signaling pathway, we further examined the mechanism underlying IFN-β induction by testing the possibility of interaction between NS5B and the TLR3 adaptor protein TRIF (Yamamoto et al., 2002). We prepared HEK/NS5B cells stably expressing myc-tagged NS5A or myc-tagged TRIF and examined whether or not NS5B interacts with TRIF by an immunoprecipitation method following Western blot analysis. The results clearly showed that NS5B and myc-tagged NS5A were co-immunoprecipitated by anti-myc antibody as reported previously (Shirota et al., 2002). However, co-immunoprecipitation of NS5B and myc-tagged TRIF was clearly not observed (Fig. 8). This result suggests that the activation of the TLR3 signaling pathway by NS5B occurs through one or more factors other than TRIF.

Induction of IFN-β depends on RNA-dependent RNA polymerase (RdRp) activity of NS5B

Since dsRNA, an intermediate of viral replication, is known as a natural ligand for the activation of TLR3 (Alexopoulou et

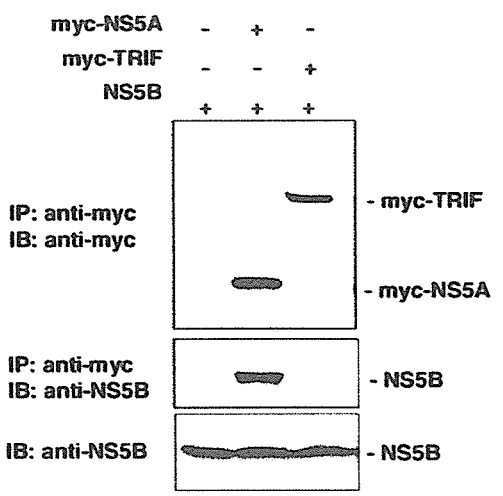

Fig. 8. NS5B does not interact with TRIF. HEK/NS5B cells were infected with pCXpur retrovirus encoding myc-tagged NS5A (middle lane) or myc-tagged TRIF (right lane). pCXpur retrovirus was used as a control infection (left lane). Cell lysate was immunoprecipitated (IP) with anti-myc antibody-conjugated agarose beads. The immunoprecipitates were resolved by SDS-PAGE, and anti-myc (upper panel) and anti-NS5B (middle panel) antibodies were used for the immunoblotting (IB) analysis. To confirm the expression level of NS5B, cell lysates were subjected to immunoblotting analysis using anti-NS5B antibody (lower panel).

al., 2001; Takeda et al., 2003), we next examined whether or not the induction of IFN-β in human hepatocytes expressing NS5B (591 amino acids; amino acids 2420 to 3010 in the HCV-1b genotype) (Kato et al., 1990) depends on NS5B's RdRp activity. Since this activity is already well characterized (Hagedorn et al., 2000), we constructed several NS5B mutants to evaluate this subject (Fig. 9A). One is the substitution mutant G2736V of the GDD motif (amino acids 2736–8) located in the catalytic site, and the other is the deletion mutant Δ2575–7 (R2753T, K2754S, and Δ2575–7) at the priming and interrogation sites, all of which are essential for NS5B's RdRp activity (Behrens et al., 1996; Bressanelli et al., 2002). We also constructed three carboxyl-truncated forms (ΔC21, ΔC56, and ΔC97, lacking 21, 56, and 97 amino acids, respectively) of NS5B. These truncated mutants of NS5B lack the last 21 hydrophobic amino acids, which are necessary and sufficient to target NS5B to the cytosolic side of the endoplasmic reticulum (ER) membrane (Schmidt-Mende et al., 2001; Yamashita et al., 1998). Although ΔC21 and ΔC56, but not ΔC97, possess RdRp activity in vitro, ΔC56 shows higher RdRp activity than ΔC21 because only the latter possesses a regulatory motif inhibiting RNA binding and polymerase activity (Leveque et al., 2003). We prepared PH5CH8 cells stably expressing these NS5B mutants and then performed cell cycle analysis using these

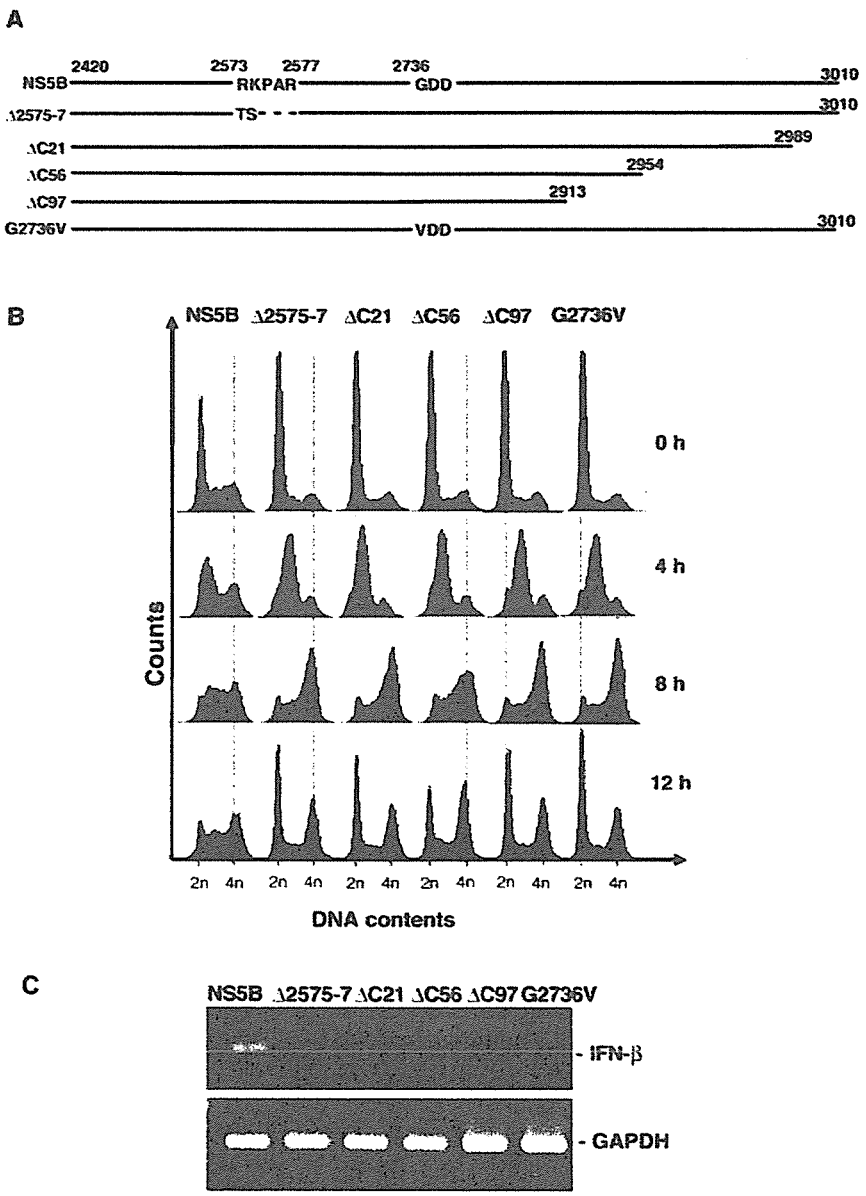

Fig. 9. The RdRp activity of NS5B anchoring on ER membrane is required for induction of IFN-β and following the delay of S phase progression. (A) Schematic presentation of the NS5B mutants used. Only amino acid sequences in the mutated regions of NS5B are indicated. (B) Cell cycle analysis of PH/NS5B and PH5CH8 cells expressing NS5B mutants. Cell cycle distribution was analyzed as described in Fig. 1B. (C) RT-PCR analysis of IFN-β mRNA in PH/NS5B and PH5CH8 cells expressing NS5B mutants. RT-PCR analysis was performed as described in Fig. 3A.

prepared cells. The results revealed no effect on S phase progression in the PH5CH8 cells expressing NS5B mutants (Fig. 9B), although PH5CH8 cells expressing ΔC56 showed a slight delay of S phase progression. Induction of IFN-β mRNA was also not observed in the PH5CH8 cells expressing NS5B mutants (Fig. 9C). These results revealed that the delay of S phase progression and the induction of IFN-β depend on the RdRp activity of NS5B, and these effects are coupled with ER membrane anchorage of NS5B in cells.

To examine the activation of IRF3, a factor specifically induced by stimulated TLR3 or TLR4, by the expression of NS5B and its mutants, we performed a dual-luciferase reporter assay using a synthetic promoter having five repeats of the consensus ISRE, which was the same as the IRF3 target sequence in the *IFN-β* gene promoter (Fig. 10A) and an intrinsic *IFN-β* gene promoter (Fig. 10B). The results showed that the luciferase activity was enhanced approximately five-fold (Fig. 10A) and eight-fold (Fig. 10B) only in PH/NS5B cells,

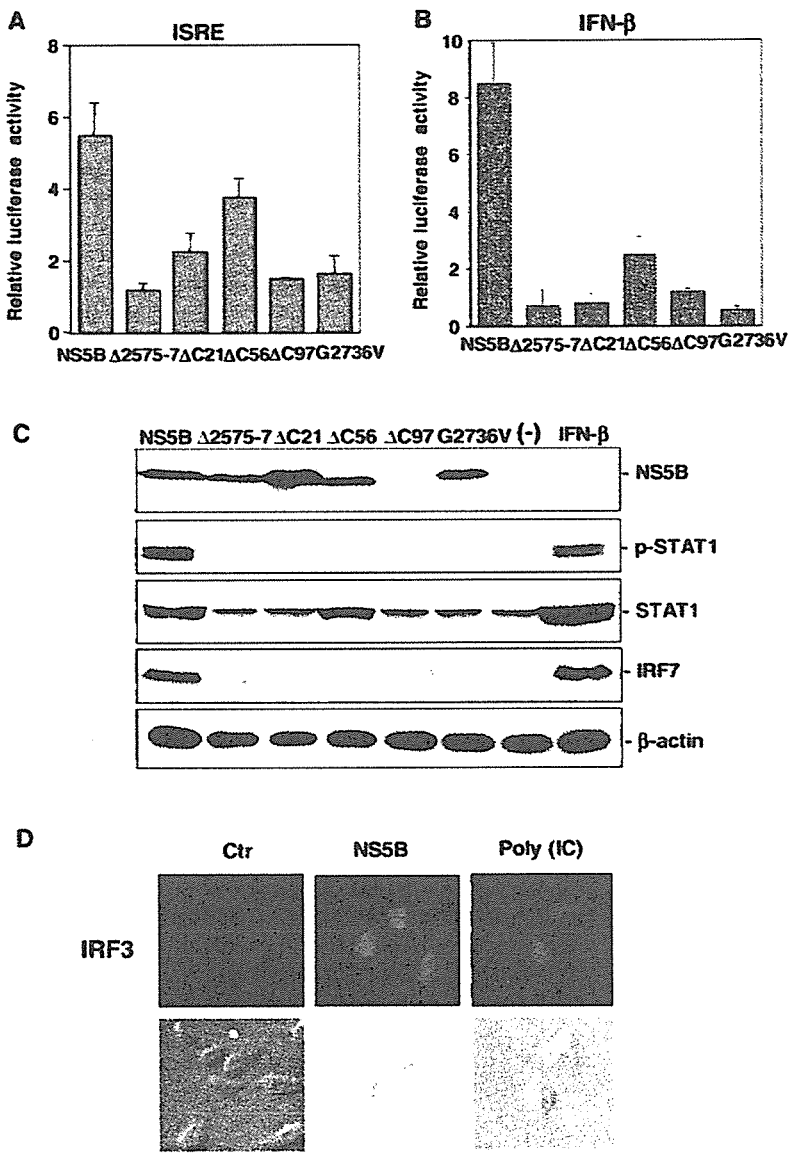

Fig. 10. NS5B full form is required for activation of IRF3 target sequences and IFN-β signaling pathway. (A) Dual luciferase reporter assay toward IRF3 target sequences. PH5CH8 cells were transfected with the pISRE-Luc (Stratagene) and pCXbsr encoding NS5B or its mutant, and the dual luciferase assay was performed as indicated in Fig. 6B. The lysates of cells transfected with pCXbsr were used as a control. (B) Dual luciferase reporter assay of the IFN-β gene promoter. Dual luciferase assay was performed as described in panel A except using pIFN-β(-125)-Luc instead of pISRE-Luc. (C) Western blot analysis of the components involved in the IFN-β signaling pathway. The lysates of PH/NS5B and PH5CH8 cells expressing NS5B mutants were subjected to immunoblotting using anti-NS5B, anti-p-STAT1(Y701), anti-STAT1, anti-IRF7, and anti-β-actin antibodies. PH5CH8 cells treated with or without IFN-β (500 IU/ml for 24 h) were also analyzed as a control. (D) Subcellular distribution of endogenous IRF3. PH/Ctr and PH/NS5B cells were processed and stained with anti-IRF3 antibody and an FITC-conjugated secondary antibody. PH5CH8 cells treated with poly (IC) were also used as a positive control.

suggesting that IRF3 is activated by the NS5B full form. Interestingly, however, luciferase activity was enhanced approximately four-fold (Fig. 10A) and three-fold (Fig. 10B) in PH5CH8 cells expressing ΔC56, although the enhancement was not as great as the five-fold (Fig. 10A) and eight-fold (Fig. 10B) in PH/NS5B cells, respectively. We then examined the phosphorylation status of STAT1 on Y701 and the level of IRF7, one of the downstream targets of the IFN-β signaling pathway (Katze et al., 2002). Western blot analysis revealed marked phosphorylation of STAT1 and IRF7 expression in PH/NS5B cells as well as in PH5CH8 cells treated with IFN-β (Fig. 10C). Although slight phosphorylation of STAT1 was observed in the PH5CH8 cells expressing ΔC56, IRF7 expression was not observed (Fig. 10C). Unlike PH/NS5B cells and PH5CH8 cells expressing ΔC56, neither the phosphorylation of STAT1 nor the expression of IRF7 was detected in PH5CH8 cells expressing other NS5B mutants. These results indicated that ΔC56 had an extremely low ability to induce IFN-β after activation of TLR3, although ΔC56 was still able to enhance the IRF3 target promoter. To obtain further evidence of the activation of IRF3, we examined the subcellular distribution of endogenous IRF3 in PH/Ctr and PH/NS5B

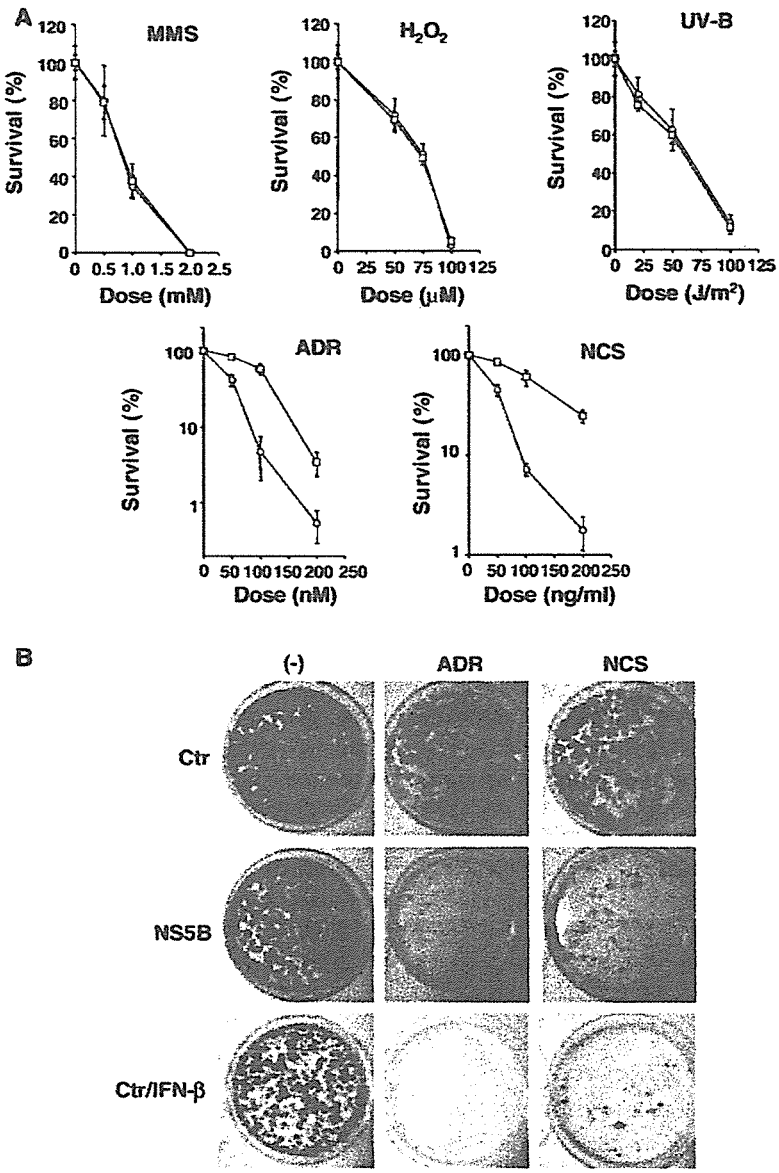

Fig. 11. Sensitivity of PH/NS5B cells against DNA-damaging reagents. (A) Clonogenic assays for PH/Ctr (square) and PH/NS5B (circle) cells after treatment with increasing doses of DNA-damaging reagents. Cells were treated with MMS, H_2O_2, UV-B, ADR, and NCS. Ten days after the treatment, cells were fixed and stained with Coomassie brilliant blue. Only colonies containing >50 cells were scored as being derived from viable clonogenic cells. Data are means ± SD from two independent triplicate experiments. (B) PH/Ctr, PH/NS5B, and IFN-β-treated (20 IU/ml) PH/Ctr cells were treated with ADR (100 nM) or NCS (100 ng/ml). The panels show survived colonies that are stained with Coomassie brilliant blue at 10 days after the treatment.

cells. In PH/Ctr cells, IRF3 was distributed in a perinuclear and/or cytoplasmic context. However, in PH/NS5B cells as well as PH5CH8 cells treated with poly (IC), IRF3 was distributed to the nucleus, a finding consistent with its activated state (Fig. 10D). Taken together, our findings indicate that the RdRp activity of HCV NS5B anchoring on ER membrane is necessary and sufficient to activate the TLR3 signaling pathway.

PH/NS5B cells are more susceptible than PH/Ctr cells to DNA-damaging reagents

To better understand the effect of IFN-β induction in PH/NS5B cells, we next examined the susceptibilities of PH/NS5B and PH/Ctr cells against various types of DNA-damaging reagents. A clonogenic assay using PH/NS5B and PH/Ctr cells was performed by treatment with MMS (a DNA alkylating reagent) and H_2O_2 (a DNA oxidative reagent) and by UV-B irradiation, which induces DNA single-strand breaks and/or thymidine dimer formation in DNA. ADR and NCS, which induce DNA double-strand breaks, were also used for the clonogenic assay. As shown in Fig. 11A, PH/NS5B and PH/Ctr cells were susceptible to the MMS treatment, the H_2O_2 treatment, and the UV-B irradiation, and no differences were observed between their susceptibilities. Interestingly, however, PH/NS5B cells were more susceptible than PH/Ctr cells against ADR or NCS treatment (Fig. 11A). These results suggest that PH/NS5B cells are more sensitive than PH/Ctr cells to damage in the form of DNA double-strand breaks. To clarify whether or not IFN-β induction increases the susceptibility against ADR or NCS treatment, we examined the effect of ADR or NCS in PH/Ctr cells treated with IFN-β. In this treatment, the cells changed to susceptible phenotype against ADR or NCS treatment, as observed in PH/NS5B cells (Fig. 11B). These results suggest that IFN-β induced by NS5B in PH5CH8 cells changes the cells into the hypersensitive phenotype, making them susceptible to DNA damage in the form of double-strand breaks.

Discussion

In the present study, we found that HCV NS5B induced IFN-β in two kinds of immortalized human hepatocyte cell lines, PH5CH8 and NKNT-3. We showed that NS5B's induction of IFN-β was mediated through the TLR3 but not the RIG-I signaling pathway. The induction of IFN-β caused the delay of cell cycle progression through the S phase in these cells. Since it has been generally known that the activation of the TLR3 signaling pathway is caused by dsRNA, a molecular pattern associated with replicating viral genomes, we first obtained data suggesting that dsRNA is generated by NS5B even without replication of the viral genome.

TLRs belong to a family of evolutionarily conserved innate immune recognition molecules, and ten members of the TLR family have been identified in human (Medzhitov, 2001; Takeda et al., 2003). TLR3 recognizes dsRNA and induces the antiviral immune responses (Alexopoulou et al., 2001; Matsumoto et al., 2002). TLR3 activates transcription factor IRF3 through TRIF, leading to IFN-β production (Oshiumi et al., 2003; Yamamoto et al., 2002, 2003). We speculated on two possible mechanisms underlying the activation of the TLR3 signaling pathway by NS5B. The first possibility is that protein–protein interaction between NS5B and TRIF is involved in the activation of the TLR3 signaling pathway. However, we failed to obtain evidence of direct interaction between NS5B and TRIF. The second possibility is that the RdRp activity of NS5B contributes to the activation of TLR3. To evaluate this hypothesis, we examined whether or not several NS5B mutants, including carboxyl-truncated mutants or an RdRp activity-defective mutant (G2736V), could induce IFN-β. The experimental data clearly showed that neither the G2736V mutant nor the carboxyl-truncated mutants could induce IFN-β. Therefore, we suggested that NS5B RdRp activity anchoring the ER membrane is critical for the activation of the TLR3 signaling pathway.

The finding that NS5B RdRp activity on the ER membrane was a critical factor for the induction of IFN-β surprised us because we expected that dsRNA, a natural ligand for TLR3, was produced in NS5B-expressing hepatocyte cells without replication of the viral RNA genome. Therefore, we now presume a daring hypothesis: that NS5B can produce dsRNA using cellular RNA as a template on the ER membrane. Since no direct evidence has been found to support this hypothesis at this stage, further experiments are necessary to evaluate this hypothesis. For instance, if possible, the detection of newly synthesized dsRNA in NS5B-expressing cells or the detection of newly synthesized dsRNA by recombinant NS5B using cellular RNA in vitro may become positive evidence. Furthermore, since the formation of a membrane-associated replication complex is a characteristic of positive-stranded RNA viruses, including HCV (Shi et al., 2003), it will also be interesting to examine whether or not the RdRps of the other RNA viruses possess novel activity similar to that observed in this study. At least we recently detected that NS5B derived from an HCV-2a genome designated JFH-1, which produces virus particles infectious for HuH-7 cells (Wakita et al., 2005), also strongly induced IFN-β in PH5CH8 cells (Ikeda et al., unpublished data). In addition, we are not able to completely exclude the possibility that NS5B-encoding RNA, but not NS5B, specifically activates the TLR3 signaling pathway. However, this possibility is unlikely because the G2736V mutant with only one nucleotide substitution could not activate the TLR3 signaling pathway.

Since the activation of the TLR3 signaling pathway in NS5B-expressing PH5CH8 or NKNT-3 cells is considered to be due to a novel function of NS5B, it is important to clarify whether or not this function occurs in the HCV life cycle. Although HCV replicon systems carrying autonomously replicating HCV RNA genomes developed using HuH-7 (Blight et al., 2000; Ikeda et al., 2002; Lohmann et al., 1999) and HeLa (Zhu et al., 2003) cells have become powerful tools for basic studies of HCV, these systems would not be suitable to prove our hypothesis because the induction of IFN-β by NS5B was not observed in HuH-7 or HeLa cells, in which the TLR3 signaling pathway was suggested to be defective. In fact, it has been recently reported that HuH-7 cells lack a TLR3

response to external dsRNA (Lanford et al., 2003). Therefore, a new HCV replicon system needs to be developed using other human cell lines possessing intact TLR3 signaling pathways. We are currently making a trial to establish an HCV replicon system using PH5CH8 or NKNT-3 cells.

On the other hand, it has been recently found that an HCV serine protease, NS3-4A, can block the phosphorylation and effector action of IRF3 (Foy et al., 2003). This finding using HuH-7 cells suggests that NS3-4A mediates the proteolysis of cellular proteins within an antiviral signaling pathway upstream of IRF3, leading to persistent viral infection. The recently identified TRIF (Li et al., 2005a, 2005b) and RIG-I (Foy et al., 2005) are possible candidates for these cellular proteins. Therefore, it was thought that IFN-β induction by NS5B through the activation of TLR3 might be suppressed by NS3-4A in PH5CH8 cells. In fact, our recent study showed that NS3-4A, in a serine protease activity-dependent manner, suppressed NS5B's activation of the IFN system (Dansako et al., 2005). However, the synergistic induction of IFN-β in PH5CH8 cells co-expressing Core and NS5B was only partially suppressed by NS3-4A, whereas the induction of IFN-β by NS5B only was drastically suppressed by NS3-4A (Dansako et al., 2005). We speculate that a biological implication of this phenomenon is that HCV proteins contribute to the maintenance of a low steady state of the virus by controlling the expression level of IFN-β in the infected cells.

In addition to the delay of cell cycle progression through the S phase, enhanced susceptibility to DNA-damaging reagents was found in NS5B-expressing PH5CH8 cells. This phenomenon was attributed to IFN-β induced by NS5B. Further characterization of this phenomenon may contribute to the understanding of IFN-β's biological effects on hepatocytes and effects on the pathogenesis of hepatocellular carcinoma caused by HCV. Furthermore, the findings of the present study may contribute to an understanding of the mechanisms underlying the TLR3 activation involved in innate immunity against viral infection. In addition, our findings suggest that an antiviral state in uninfected cells may be induced by the expression of a viral protein, NS5B.

Materials and methods

Cell culture and cell cycle analysis

The non-neoplastic immortalized human hepatocyte cell lines, PH5CH8 and NKNT-3 cells, were maintained as described previously (Ikeda et al., 1998; Kobayashi et al., 2000). Human hepatoma cell line HuH-7 cells, human cervical carcinoma HeLa cells, and HEK 293 cells were cultured in Dulbecco's modified Eagle's medium supplemented with 10% fetal bovine serum.

To synchronize the cells at the G1/S transition, growing cells were treated with thymidine (Sigma, St. Louis, MO) (2.5 mM) for 19 h, washed in PBS, and released into fresh medium for 11 h. The cells were then treated with aphidicolin (Sigma) (5 μM) for 13 h, washed in PBS, and released into fresh medium. The cells were pulse-labeled with 10 μM bromodeoxyuridine (BrdUrd; Sigma) for 1 h, fixed with 70% ethanol at indicated time points, stained with fluorescein-isothiocyanate (FITC)-conjugated mouse monoclonal antibody to BrdUrd (BD Pharmingen, San Diego, CA), and counterstained with propidium iodide (PI) (Sigma). The cellular content of DNA was determined by flow cytometry with FACScalibur instrument, and data were analyzed with CELL Quest software (BD Biosciences, San Jose, CA) (Naka et al., 2004). To determine the population of G2-M phase reached cells, the cells were treated with Nocodazole (Noc; Sigma) (200 ng/ml) at 5 h after release into the S phase. Then, after 7 h (post release from 12 h), the cell population that had accumulated in the G2-M phase was analyzed by flow cytometry. To examine the effects of IFN-β, PH5CH8 and NKNT-3 cells were treated with or without IFN-β (500 IU/ml) at 12 h prior to release, and cell cycle progression was analyzed. To assess the effect of anti-IFN-β neutralizing antibody, NS5B-expressing cells were treated with anti-IFN-β antibody (70 U/ml, OBT0377, Oxford Biotechnology, Oxfordshire, UK) during cell cycle synchronization and after release from the G1/S boundary.

Vector construction and retrovirus infection

Retroviral vectors pCXbsr (Akagi et al., 2000) and pCX4bsr (Akagi et al., 2003), which contain the resistance gene for blasticidin, were used in this study. The DNA fragments encoding the influenza hemagglutinin tagged (HA)-core, NS3, HA-NS4B, HA-NS5A, HA-NS5B, and NS5B were amplified from pMILE (HCV 1B-1 strain belonging to genotype 1b; accession no. AB080299) by PCR using KOD-plus DNA polymerase (Toyobo, Osaka, Japan). The obtained DNA fragments were subcloned into the *Eco*RI (*Bam*HI for NS5B) and *Not*I sites of pCXbsr or pCX4bsr. The DNA fragment encoding myc-tagged NS5A was also amplified from pMILE by PCR. The obtained DNA fragment was subcloned into the *Eco*RI and *Not*I sites of pCXpur (Akagi et al., 2000), which contains the resistance gene for puromycin. The DNA fragments encoding TLR3 (accession no. NM_003265), Toll-IL-1 receptor (TIR) domain-containing adaptor-inducing IFN-β (TRIF or TICAM-1, accession no. NM_182919), and RIG-IC, a dominant negative inhibitor of retinoic acid-inducible gene-I (RIG-I) (Yoneyama et al., 2004), were amplified from cDNAs obtained from PH5CH8 cells. The primer sequences containing the *Sph*I (for forward) or *Not*I (for reverse) recognition sites for TLR3, TRIF, and RIG-IC were designed to enable expression of the TLR3, TRIF, and RIG-IC open-reading frames, respectively. The obtained DNA fragments were subcloned into the *Sph*I and *Not*I sites of pCXpur/myc, which can express myc-tagged protein. The *IFN-β* gene promoter region (−125 to +19) described previously (Fujita et al., 1988) was amplified using genomic DNA derived from PH5CH8 cells and a primer set of 5′-ACGGGGTACC-GAGTTTTAGAAACTACTAAAATG-3′ containing the *Kpn*I recognition site (underlined) and 5′-AGGAAGATCTTC-GAAAGGTTGCAGTTAGAATG-3′ containing the *Bgl*II recognition site (underlined). The obtained DNA fragment was

subcloned into the *Kpn*I and *Bgl*II sites of pGL3-Basic (Promega) and was termed pIFN-β(-125)-Luc. Retrovirus infections were performed as described previously (Naganuma et al., 2004).

RT-PCR and RNA interference

RT-PCR was carried out as described previously (Dansako et al., 2003). The sequences of sense and antisense primers for IFN-β (accession no. V00547) were 5′-CCCTGAGGAGATTAAGCAGCTGC-3′ and 5′-AGTTCCTTAGGATTTCCACTCTGAC-3′. The sequences of primer set for ISG56 (accession no. X03557) were 5′-AGAAGCAGGCAATCACAGAAAAGCTG-3′ and 5′-CCAGGGCTTCATTCATATTTCCTTCC-3′. Small-interference RNA (siRNA) duplexes targeting the coding regions of human TLR3, TLR4, and luciferase GL2 (Elbashir et al., 2001) as a control were chemically synthesized (Greiner, Tokyo, Japan). The sequences of the human TLR3 oligonucleotides were: 5′-CCUCCAGCACAAUGAGCUATT-3′ and 5′-UAGCUCAUUGUGCUGGAGGTT-3′. The sequences of the human TLR4 oligonucleotides were: 5′-CCUCCCCUUCUCAACCAAGTT-3′ and 5′-CUUGGUUGAGAAGGGGAGGTT-3′. The cells were transfected with the indicated siRNA duplex using OligofectAMINE (Invitrogen, Carlsbad, CA). Total RNAs were extracted after 3 days, and RT-PCR was performed using primer sets for TLR3 (Kadowaki et al., 2001), TLR4 (Kadowaki et al., 2001), and GAPDH (Dansako et al., 2003).

Western blot analysis

The preparation of cell lysates, SDS-PAGE, and immunoblotting analysis were performed according to standard procedures using primary antibodies, rat monoclonal anti-HA (3F10; Roche Molecular Biochemicals, Mannheim, Germany), mouse monoclonal anti-NS3 (clone MMM33; Novacastra Laboratories, Newcastle upon Tyne, UK), anti-NS5B (a gift from Dr. M. Kohara), anti-myc (PL14; Medical and biological laboratories, Nagoya, Japan), anti-β-actin (AC-15, Sigma), anti-STAT1 (clone 42; BD Transduction Laboratories, San Diego, CA), rabbit polyclonal anti-phospho-STAT1(Y701) (Cell Signaling Technology, Beverly, MA), and anti-IRF7 (H-246, Santa Cruz Biotechnology, Santa Cruz, CA), and horseradish-peroxidase-conjugated secondary antibodies. The immune complex was visualized using the ECL Western blot detection system (Amersham Bioscience, Piscataway, NJ).

Reporter assay

The luciferase activity was measured by dual-luciferase assay system (Promega, Madison, WI) as previously described (Dansako et al., 2003). Briefly, cells were transfected with pISRE-Luc (Stratagene, LaJolla, CA) or pIFN-β(-125)-Luc reporter plasmid together with phRL-CMV (Promega) as an internal control reporter plasmid by FuGENE6 (Roche). After 48 h of transfection, cell lysates were then prepared and assayed for luciferase activities; transfection efficiency was normalized by renilla luciferase activity (internal control) derived from phRL-CMV. Three independent triplicate transfection experiments were conducted in order to verify the reproducibly of the results.

Immunoprecipitation

Cells were lysed in a buffer containing 50 mM Tris (pH 7.4), 125 mM NaCl, 0.1%(v/v) Nonidet P-40 (NP-40; Sigma), 5 mM EDTA, 0.1 M NaF, and a mixture of protease inhibitors (Complete; Roche). Pre-cleared cell lysates were subjected to immunoprecipitation using agarose-conjugated anti-myc antibody (PL14, MBL). Bound proteins were eluted from beads by boiling in SDS sample buffer, and immunoblotting analysis was performed using anti-myc or anti-NS5B antibody, and HRP-conjugated anti-mouse IgG TrueBlot (eBioscience, San Diego, CA).

Immunofluorescence analysis

To examine the intracellular protein localization, 2×10^4 cells were cultured and treated on chamber slides then fixed and probed with polyclonal rabbit anti-IRF3 antibody (FL-425, Santa Cruz Biotechnology) and FITC-conjugated donkey anti-rabbit secondary antibody according to a method described previously (Foy et al., 2003). PH5CH8 cells treated with poly (IC) (2.5 μg/ml for 6 h; Amersham Biosciences) were used as a positive control for the activation of IRF3.

Evaluation of sensitivity to DNA damage

Cells in an exponential growth phase were plated onto 10-cm plates (5×10^3 cells/plate) and cultured for 4 days. The cells were treated with hydrogen peroxide (H_2O_2; Wako Pure Chemical, Osaka, Japan), methylmethane sulfonate (MMS; Sigma), Adriamycin (ADR; doxorubicin; Sigma), and neocarzinostatin chromophore (NCS; generously provided by Kayaku, Tokyo, Japan) for 2 h at 37 °C. For UV-B treatment (UV-B radiation at 302 nm), the medium was aspirated prior to exposure, the cells were washed twice with PBS, and then a fresh culture medium was added. Ten days later, the cells were fixed and stained with Coomassie brilliant blue as described previously (Naganuma et al., 2004). Only colonies containing >50 cells were scored as being derived from viable clonogenic cells.

Acknowledgments

We thank Drs. M. Kohara and T. Akagi for the anti-NS5B monoclonal antibody and pCX retroviral vectors, respectively, and A. Nozaki for suggestions and comments. We also thank T. Nakamura, A. Morishita, and H. Tawara for their technical assistance. This work was supported by grants-in-aid for research on hepatitis from the Ministry of Health, Labour, and Welfare of Japan and by the program for promotion of fundamental studies in Health Sciences of the National Institute of Biomedical Innovation (NIBIO).

References

Akagi, T., Shishido, T., Murata, K., Hanafusa, H., 2000. v-Crk activates the phosphoinositide 3-kinase/AKT pathway in transformation. Proc. Natl. Acad. Sci. U.S.A. 97, 7290–7295.

Akagi, T., Sasai, K., Hanafusa, H., 2003. Refractory nature of normal human diploid fibroblasts with respect to oncogene-mediated transformation. Proc. Natl. Acad. Sci. U.S.A. 100, 13567–13572.

Alexopoulou, L., Holt, A.C., Medzhitov, R., Flavell, R.A., 2001. Recognition of double-stranded RNA and activation of NF-kappaB by Toll-like receptor 3. Nature 413, 732–738.

Arima, N., Kao, C.Y., Licht, T., Padmanabhan, R., Sasaguri, Y., 2001. Modulation of cell growth by the hepatitis C virus nonstructural protein NS5A. J. Biol. Chem. 276, 12675–12684.

Bartenschlager, R., Lohmann, V., 2000. Replication of hepatitis C virus. J. Gen. Virol. 81, 1631–1648.

Behrens, S.E., Tomei, L., De Francesco, R., 1996. Identification and properties of the RNA-dependent RNA polymerase of hepatitis C virus. EMBO J. 15, 12–22.

Blight, K.J., Kolykhalov, A.A., Rice, C.M., 2000. Efficient initiation of HCV RNA replication in cell culture. Science 290, 1972–1974.

Bressanelli, S., Tomei, L., Rey, F.A., De Francesco, R., 2002. Structural analysis of the hepatitis C virus RNA polymerase in complex with ribonucleotides. J. Virol. 76, 3482–3492.

Colombo, M., 1996. The natural history of hepatitis C. Bailliere's Clin. Gastroenterol. 10, 275–288.

Dansako, H., Naganuma, A., Nakamura, T., Ikeda, F., Nozaki, A., Kato, N., 2003. Differential activation of interferon-inducible genes by hepatitis C virus core protein mediated by the interferon stimulated response element. Virus Res. 97, 17–30.

Dansako, H., Naka, K., Ikeda, M., Kato, N., 2005. Hepatitis C virus proteins exhibit conflicting effects on the interferon system in human hepatocyte cells. Biochem. Biophys. Res. Commun. 336, 458–469.

Dore, M.P., Realdi, G., Mura, D., Onida, A., Massarelli, G., Dettori, G., Graham, D.Y., Sepulveda, A.R., 2001. Genomic instability in chronic viral hepatitis and hepatocellular carcinoma. Hum. Pathol. 32, 698–703.

Dubourdeau, M., Miyamura, T., Matsuura, Y., Alric, L., Pipy, B., Rousseau, D., 2002. Infection of HepG2 cells with recombinant adenovirus encoding the HCV core protein induces p21(WAF1) down-regulation—Effect of transforming growth factor beta. J. Hepatol. 37, 486–492.

Elbashir, S.M., Harborth, J., Lendeckel, W., Yalcin, A., Weber, K., Tuschl, T., 2001. Duplexes of 21-nucleotide RNAs mediate RNA interference in cultured mammalian cells. Nature 411, 494–498.

Foy, E., Li, K., Wang, C., Sumpter Jr., R., Ikeda, M., Lemon, S.M., Gale Jr., M., 2003. Regulation of interferon regulatory factor-3 by the hepatitis C virus serine protease. Science 300, 1145–1148.

Foy, E., Li, K., Sumpter Jr., R., Loo, Y.M., Johnson, C.L., Wang, C., Fish, P.M., Yoneyama, M., Fujita, T., Lemon, S.M., Gale Jr., R., 2005. Control of antiviral defenses through hepatitis C virus disruption of retinoic acid-inducible gene-I signaling. Proc. Natl. Acad. Sci. U.S.A. 102, 2986–2991.

Fujita, T., Sakakibara, J., Sudo, Y., Miyamoto, M., Kimura, Y., Taniguchi, T., 1988. Evidence for a nuclear factor(s), IRF-1, mediating induction and silencing properties to human IFN-beta gene regulatory elements. EMBO J. 7, 3397–3405.

Hagedorn, C.H., van Beers, E.H., De Staercke, C., 2000. Hepatitis C virus RNA-dependent RNA polymerase (NS5B polymerase). Curr. Top. Microbiol. Immunol. 242, 225–260.

Hsu, I.C., Tokiwa, T., Bennett, W., Metcalf, R.A., Welsh, J.A., Sun, T., Harris, C.C., 1993. p53 gene mutation and integrated hepatitis B viral DNA sequences in human liver cancer cell lines. Carcinogenesis 14, 987–992.

Ikeda, M., Sugiyama, K., Mizutani, T., Tanaka, T., Tanaka, K., Sekihara, H., Shimotohno, K., Kato, N., 1998. Human hepatocyte clonal cell lines that support persistent replication of hepatitis C virus. Virus Res. 56, 157–167.

Ikeda, M., Yi, M., Li, K., Lemon, S.M., 2002. Selectable subgenomic and genome-length dicistronic RNAs derived from an infectious molecular clone of the HCV-N strain of hepatitis C virus replicate efficiently in cultured Huh7 cells. J. Virol. 76, 2997–3006.

Jung, E.Y., Lee, M.N., Yang, H.Y., Yu, D., Jang, K.L., 2001. The repressive activity of hepatitis C virus core protein on the transcription of p21(waf1) is regulated by protein kinase A-mediated phosphorylation. Virus Res. 79, 109–115.

Kadowaki, N., Ho, S., Antonenko, S., Malefyt, R.W., Kastelein, R.A., Bazan, F., Liu, Y.J., 2001. Subsets of human dendritic cell precursors express different toll-like receptors and respond to different microbial antigens. J. Exp. Med. 194, 863–869.

Kato, N., 2001. Molecular virology of hepatitis C virus. Acta Med. Okayama 55, 133–159.

Kato, N., Hijikata, M., Ootsuyama, Y., Nakagawa, M., Ohkoshi, S., Sugimura, T., Shimotohno, K., 1990. Molecular cloning of the human hepatitis C virus genome from Japanese patients with non-A, non-B hepatitis. Proc. Natl. Acad. Sci. U.S.A. 87, 9524–9528.

Katze, M.G., He, Y., Gale Jr., M., 2002. Viruses and interferon: a fight for supremacy. Nat. Rev., Immunol. 2, 675–687.

Kobayashi, N., Fujiwara, T., Westerman, K.A., Inoue, Y., Sakaguchi, M., Noguchi, H., Miyazaki, M., Cai, J., Tanaka, N., Fox, I.J., Leboulch, P., 2000. Prevention of acute liver failure in rats with reversibly immortalized human hepatocytes. Science 287, 1258–1262.

Kondo, Y., Kanai, Y., Sakamoto, M., Mizokami, M., Ueda, R., Hirohashi, S., 2000. Genetic instability and aberrant DNA methylation in chronic hepatitis and cirrhosis-A comprehensive study of loss of heterozygosity and microsatellite instability at 39 loci and DNA hypermethylation on 8 CpG islands in microdissected specimens from patients with hepatocellular carcinoma. Hepatology 32, 970–979.

Lanford, R.E., Guerra, B., Lee, H., Averett, D.R., Pfeiffer, B., Chavez, D., Notvall, L., Bigger, C., 2003. Antiviral effect and virus–host interactions in response to alpha interferon, gamma interferon, poly(i)-poly(c), tumor necrosis factor alpha, and ribavirin in hepatitis C virus subgenomic replicons. J. Virol. 77, 1092–1104.

Leveque, V.J., Johnson, R.B., Parsons, S., Ren, J., Xie, C., Zhang, F., Wang, Q.M., 2003. Identification of a C-terminal regulatory motif in hepatitis C virus RNA-dependent RNA polymerase: structural and biochemical analysis. J. Virol. 77, 9020–9028.

Li, K., Chen, Z., Kato, N., Gale Jr., M., Lemon, S.M., 2005a. Distinct poly(I-C) and virus-activated signaling pathways leading to interferon-β production in hepatocytes. J. Biol. Chem. 280, 16739–16747.

Li, K., Foy, E., Ferreon, J.C., Nakamura, M., Ferreon, A.C.M., Ikeda, M., Ray, S.C., Gale Jr., M., Lemon, S.M., 2005b. Immune evasion by hepatitis C virus NS3/4A protease-mediated cleavage of the Toll-like receptor-3 adaptor protein, TRIF. Proc. Natl. Acad. Sci. U.S.A. 102, 2992–2997.

Lohmann, V., Korner, F., Koch, J., Herian, U., Theilmann, L., Bartenschlager, R., 1999. Replication of subgenomic hepatitis C virus RNAs in a hepatoma cell line. Science 285, 110–113.

Lu, W., Lo, S.Y., Chen, M., Wu, K., Fung, Y.K., Ou, J.H., 1999. Activation of p53 tumor suppressor by hepatitis C virus core protein. Virology 264, 134–141.

Marusawa, H., Hijikata, M., Chiba, T., Shimotohno, K., 1999. Hepatitis C virus core protein inhibits Fas- and tumor necrosis factor alpha-mediated apoptosis via NF-kappaB activation. J. Virol. 73, 4713–4720.

Matsumoto, M., Kikkawa, S., Kohase, M., Miyake, K., Seya, T., 2002. Establishment of a monoclonal antibody against human Toll-like receptor 3 that blocks double-stranded RNA-mediated signaling. Biochem. Biophys. Res. Commun. 293, 1364–1369.

Medzhitov, R., 2001. Toll-like receptors and innate immunity. Nat. Rev., Immunol. 1, 135–145.

Naganuma, A., Nozaki, A., Tanaka, T., Sugiyama, K., Takagi, H., Mori, M., Shimotohno, K., Kato, N., 2000. Activation of the interferon-inducible 2'-5'-oligoadenylate synthetase gene by hepatitis C virus core protein. J. Virol. 74, 8744–8750.

Naganuma, A., Dansako, H., Nakamura, T., Nozaki, A., Kato, N., 2004. Disturbance of the DNA repair system by HCV core protein. Cancer Res. 64, 1307–1314.

Naka, K., Tachibana, A., Ikeda, K., Motoyama, N., 2004. Stress-induced premature senescence in hTERT-expressing ataxia telangiectasia fibroblasts. J. Biol. Chem. 279, 2030–2037.

Noguchi, M., Hirohashi, S., 1996. Cell lines from non-neoplastic liver and hepatocellular carcinoma tissue from a single patient. In Vitro Cell. Dev. Biol. 32, 135–137.

Oshiumi, H., Matsumoto, M., Funami, K., Akazawa, T., Seya, T., 2003. TICAM-1, an adaptor molecule that participates in Toll-like receptor 3-mediated interferon-beta induction. Nat. Immunol. 4, 161–167.

Ray, R.B., Ray, R., 2001. Hepatitis C virus core protein: intriguing properties and functional relevance. FEMS Microbiol. Lett. 202, 149–156.

Ray, R.B., Steele, R., Meyer, K., Ray, R., 1998. Hepatitis C virus core protein represses p21WAF1/Cip1/Sid1 promoter activity. Gene 208, 331–336.

Reed, K.E., Rice, C.M., 2000. Overview of hepatitis C virus genome structure, polyprotein processing, and protein properties. Curr. Top. Microbiol. Immunol. 242, 55–84.

Schmidt-Mende, J., Bieck, E., Hugle, T., Penin, F., Rice, C.M., Blum, H.E., Moradpour, D., 2001. Determinants for membrane association of the hepatitis C virus RNA-dependent RNA polymerase. J. Biol. Chem. 276, 44052–44063.

Scholle, F., Li, K., Bodola, F., Ikeda, M., Luxon, B.A., Lemon, S.M., 2004. Virus–host cell interactions during hepatitis C virus RNA replication: impact of polyprotein expression on the cellular transcriptome and cell cycle association with viral RNA synthesis. J. Virol. 78, 1513–1524.

Shi, S.T., Lee, K.J., Aizaki, H., Hwang, S.B., Lai, M.M., 2003. Hepatitis C virus RNA replication occurs on a detergent-resistant membrane that cofractionates with caveolin-2. J. Virol. 77, 4160–4168.

Shirota, Y., Luo, H., Qin, W., Kaneko, S., Yamashita, T., Kobayashi, K., Murakami, S., 2002. Hepatitis C virus (HCV) NS5A binds RNA-dependent RNA polymerase (RdRP) NS5B and modulates RNA-dependent RNA polymerase activity. J. Biol. Chem. 277, 11149–11155.

Takeda, K., Kaisho, T., Akira, S., 2003. Toll-like receptors. Annu. Rev. Immunol. 21, 335–376.

Thomas, D.L., 2000. Hepatitis C epidemiology. Curr. Top. Microbiol. Immunol. 242, 25–41.

Tsuchihara, K., Hijikata, M., Fukuda, K., Kuroki, T., Yamamoto, N., Shimotohno, K., 1999. Hepatitis C virus core protein regulates cell growth and signal transduction pathway transmitting growth stimuli. Virology 258, 100–107.

Vannucchi, S., Percario, Z.A., Chiantore, M.V., Matarrese, P., Chelbi-Alix, M.K., Fagioli, M., Pelicci, P.G., Malomi, W., Fiorucci, G., Romeo, G., Affabris, E., 2000. Interferon-beta induces S phase slowing via up-regulated expression of PML in squamous carcinoma cells. Oncogene 19, 5041–5053.

Wakita, T., Pietschmann, T., Kato, T., Date, T., Miyamoto, M., Zhao, Z., Murthy, K., habermann, A., Krausslich, H.G., Mizokami, M., Bartenschlager, R., Liang, T.J., 2005. Production of infectious hepatitis C virus in tissue culture from a cloned viral genome. Nat. Med. 11, 791–796.

Yamamoto, M., Sato, S., Mori, K., Hoshino, K., Takeuchi, O., Takeda, K., Akira, S., 2002. Cutting edge: a novel Toll/IL-1 receptor domain-containing adapter that preferentially activates the IFN-beta promoter in the Toll-like receptor signaling. J. Immunol. 169, 6668–6672.

Yamamoto, M., Sato, S., Hemmi, H., Hoshino, K., Kaisho, T., Sanjo, H., Takeuchi, O., Sugiyama, M., Okabe, M., Takeda, K., Akira, S., 2003. Role of adaptor TRIF in the MyD88-independent toll-like receptor signaling pathway. Science 301, 640–643.

Yamashita, T., Kaneko, S., Shirota, Y., Qin, W., Nomura, T., Kobayashi, K., Murakami, S., 1998. RNA-dependent RNA polymerase activity of the soluble recombinant hepatitis C virus NS5B protein truncated at the C-terminal region. J. Biol. Chem. 273, 15479–15486.

Yoneyama, M., Kikuchi, M., Natsukawa, T., Shinobu, N., Imaizumi, T., Miyagishi, M., Taira, K., Akira, S., Fujita, T., 2004. The RNA helicase RIG-I has an essential function in double-stranded RNA-induced innate antiviral responses. Nat. Immunol. 5, 730–737.

Zhu, Q., Guo, J.T., Seeger, C., 2003. Replication of hepatitis C virus subgenomes in nonhepatic epithelial and mouse hepatoma cells. J. Virol. 77, 9204–9210.

Different Anti-HCV Profiles of Statins and Their Potential for Combination Therapy With Interferon

Masanori Ikeda, Ken-ichi Abe, Masashi Yamada, Hiromichi Dansako, Kazuhito Naka, and Nobuyuki Kato

We recently developed a genome-length hepatitis C virus (HCV) RNA replication system (OR6) with luciferase as a reporter. The OR6 assay system has enabled prompt and precise quantification of HCV RNA replication. Pegylated interferon (IFN) and ribavirin combination therapy is the world standard for chronic hepatitis C, but its effectiveness is limited to about 55% of patients. Newer therapeutic approaches are needed. In the present study, we used the OR6 assay system to evaluate the anti-HCV activity of 3-hydroxy-3-methylglutaryl coenzyme A (HMG-CoA) reductase inhibitors, called statins, and their effects in combination with IFN-α. Five types of statins (atorvastatin, fluvastatin, lovastatin, pravastatin, and simvastatin) were examined for their anti-HCV activities. Fluvastatin exhibited the strongest anti-HCV activity (IC_{50}: 0.9 μmol/L), whereas atorvastatin and simvastatin showed moderate inhibitory effects. However, lovastatin, reported recently as an inhibitor of HCV replication, was shown to exhibit the weakest anti-HCV activity. The anti-HCV activities of statins were reversed by the addition of mevalonate or geranylgeraniol. Surprisingly, however, pravastatin exhibited no anti-HCV activity, although it worked as an inhibitor for HMG-CoA reductase. The combination of IFN and the statins (except for pravastatin) exhibited strong inhibitory effects on HCV RNA replication. In combination with IFN, fluvastatin also exhibited a synergistic inhibitory effect. In conclusion, statins, especially fluvastatin, could be potentially useful as new anti-HCV reagents in combination with IFN. (HEPATOLOGY 2006;44:117-125.)

Persistent hepatitis C virus (HCV) infection causes liver fibrosis and hepatocellular carcinoma. Approximately 170 million people worldwide are infected with HCV. The combination of pegylated interferon (IFN) with ribavirin is the current standard therapy for chronic hepatitis C (CHC) and yields a sustained virological response (SVR) rate of about 55%.[1] This means that about 45% of patients with CH C are still threatened by the progression of the disease to cirrhosis and hepatocellular carcinoma. Until 1999, when Lohmann et al. developed the subgenomic replicon of HCV, it was difficult to screen anti-HCV reagents.[2] Many improvements followed that breakthrough, such as a genome-length HCV RNA replication system[3,4] and a subgenomic replicon with a reporter assay system[5]; more recently, Wakita et al. used a genotype 2a strain, JFH1, to produce the infectious virus in cell culture.[6-8]

Genotype 1 is the major genotype of HCV found in Japan, the United States, and many other countries. Unfortunately, the SVR rate after combination therapy of pegylated IFN with ribavirin is less than 50% for this genotype. To find a more effective therapy especially for CHC patients with genotype 1, we recently developed a genome-length HCV RNA (strain O of genotype 1b) replication reporter system (OR6), which has been an effective screening tool.[9,10]

Statins, which are 3-hydroxy-3-methylglutaryl coenzyme A (HMG-CoA) reductase inhibitors, are in wide use for the treatment of hypercholesterolemia. Recently, it

Abbreviations: HCV, hepatitis C virus; IFN, interferon; CHC, chronic hepatitis C; SVR, sustained virological response; HMG-CoA, 3-hydroxy-3-methylglutaryl coenzyme A; 2'-5'-OAS1, 2'-5'-oligoadenylate synthetase 1; LOV, lovastatin; ATV, atorvastatin; PRV, pravastatin; SMV, simvastatin; FLV, fluvastatin; RL, renilla luciferase; LST-1, human liver-specific organic anion transporter-1; GAPDH, glyceraldehyde 3-phosphate dehydrogenase; EMCV, encephalomyocarditis virus; IRES, internal ribosome entry site; AMPH-B, amphotericin B; RT-PCR, reverse-transcription polymerase chain reaction.

From the Department of Molecular Biology, Okayama University Graduate School of Medicine, Dentistry, and Pharmaceutical Sciences, Okayama, Japan.

Received November 17, 2005; accepted April 17, 2006.

Supported by a grant-in-aid for the third-term comprehensive 10-year strategy for cancer control and by a grant-in-aid for research on hepatitis, both from the Ministry of Health, Labor, and Welfare of Japan, and by the Program for the Promotion of Fundamental Studies in Health Science of the Pharmaceutical and Medical Device Agency (PMAD), Japan.

Address reprint requests to: Nobuyuki Kato, Ph.D., Department of Molecular Biology, Okayama University Graduate School of Medicine, Dentistry, and Pharmaceutical Sciences, 2-5-1 Shikata-cho, Okayama 700-8558, Japan. E-mail: nkato@md.okayama-u.ac.jp; fax: (81) 86-235-7392.

Published online in Wiley InterScience (www.interscience.wiley.com).

DOI 10.1002/hep.21232

Potential conflict of interest: Nothing to report.

was reported that lovastatin (LOV) inhibited HCV RNA replication.[11,12] These reports suggested the anti-HCV activity of LOV resulted from inhibition of the geranylgeranylation of cellular proteins rather than the inhibition of cholesterol synthesis.[11,12] More recently, FBL2 has been reported to be a host target protein for geranylgeranylation, which is responsible for HCV replication.[13] Although several types of statins are used clinically to lower cholesterol, thus far only LOV has been tested for anti-HCV activity. In the present study, we used the OR6 assay system to test the anti-HCV activity of five statins: atorvastatin (ATV), fluvastatin (FLV), pravastatin (PRV), simvastatin (SMV), and LOV. We found that ATV, FLV, and SMV exhibited stronger anti-HCV activity than that previously reported for LOV and that PRV exhibited no anti-HCV activity, although it worked as an inhibitor for HMG-CoA reductase. Because FLV showed the strongest anti-HCV activity, we also examined the effect of the combination of IFN-α and FLV on HCV RNA replication and found a synergistic inhibitory effect of IFN-α and FLV on HCV RNA replication.

Materials and Methods

Cell Cultures. OR6 cells were cultured in Dulbecco's modified Eagle's medium supplemented with 10% fetal calf serum, penicillin, streptomycin, and G418 (300 μg/mL; Geneticin, Invitrogen) and passaged twice a week at a 5:1 split ratio. OR6c cells are cured OR6 cells from which genome-length HCV RNA was eliminated by IFN-α treatment (500 IU/mL for 2 weeks) without G418, as previously described.[9] HepG2 and PH5CH8 (human immortalized hepatocytes) cells were cultured as previously described.[14,15]

Luciferase Reporter Assay. For the renilla luciferase (RL) assay, 2×10^4 OR6 cells were plated in 24-well plates at least in triplicate for each assay and were cultured for 24 hours. The cells were treated with statins for 72 hours and were harvested with Renilla lysis reagent (Promega) and subjected to the RL assay according to the manufacturer's protocol.

Reagents. FLV, LOV, and PRV were purchased from Calbiochem. ATV and SMV were purchased from Astellas Pharma Inc. and Banyu Pharmaceutical Co. Ltd., respectively. Mevalonate, geranylgeraniol, and geranylgeranyl pyrophosphate were purchased from Sigma.

Reverse-Transcriptase Polymerase Chain Reaction. Total RNA from the cultured cells was extracted with the RNeasy Mini Kit (Qiagen). Reverse-transcriptase polymerase chain reaction (RT-PCR) for HMG-CoA reductase, human liver-specific organic anion transporter (LST-1), 2′-5′-oligoadenylate synthetase 1 (2′-5′-OAS1), and glyceraldehyde-3-phosphate dehydrogenase (GAPDH) was performed by a method described previously.[16] Briefly, using cellular total RNA (2 μg), cDNA was synthesized using Superscript II with oligo dT primer. One-tenth of the synthesized cDNA was subjected to polymerase chain reaction (PCR) with the following primer pairs: HMG-CoA reductase, 5′-ATGCCATCCCTGTTGGAGTG-3′ and 5′-TGTTCATCCCCATGGCATCCC-3′; LST-1, 5′-TGGCACACGTGGGTCATGTAGG-3′ and 5′-CACTATCTGCCCCAGCAGAAGG-3′, 2′-5′-OAS1, 5′-AGTACCTGAGAAGGCAGCTCACGA-3′ and 5′-ACTGGCATTCAGAGGATGGTGCAG-3′; and GAPDH, 5′-GACTCATGACCACAGTCCATGC-3′, and 5′-GAGGAGACCACCTGGTGCTCAG-3′.

Western Blot Analysis. Preparation of the cell lysate, sodium dodecyl sulfate–polyacrylamide gel electrophoresis, and immunoblotting were performed as previously described.[17] The antibodies used in this study were those against Core (Institute of Immunology, Tokyo), NS3 (Novocastra Laboratories, Newcastle upon Tyne, UK), NS5B (a generous gift from Dr. M. Kohara, Tokyo Metropolitan Institute of Medical Science), β-actin (Sigma, St. Louis, MO), STAT1 (BD Transduction Laboratories, San Diego, CA), and phospho-STAT1 (Y701; Cell Signaling Technology, Beverly, MA). Immunocomplexes on the membranes were detected by the enhanced chemiluminescence assay (Renaissance; Perkin Elmer Life Science, Wellesley, MA).

Plasmid Construction. The plasmids pORN/C-5B/KE (Fig. 1A) and pHCV-O were described previously.[9] To construct the pEMCV-RL, two fragments, the encephalomyocarditis virus (EMCV) internal ribosome entry site (IRES) and the *RL* gene, were amplified by PCR from pORN/C-5B/KE using the following primer pairs: EMCV IRES, 5′-CGGGATCCGCGGGACTCGGGGGTTCG-3′ and 5′-CCGCTCGAGGGTATTATCGTGTTTTTCAAAGG-3′; and RL, 5′-CCGCTCGAGATGGCTTCCAAGGTGTACGACC-3′, and 5′-GCTCTAGACTAGACGTTGATCCTGGCGC-3′. The two fragments were ligated into the *Bam*HI and *Xba*I sites in pcDNA 3.1/Zeo (Invitrogen).

Statistical Analysis. Differences in anti-HCV activity between statins were tested using the Student t test. P values $< .05$ were considered statistically significant.

Results

Inhibition of HCV RNA Replication by Statins. We recently developed a genome-length HCV RNA (strain O of genotype 1b) replication system (OR6) with luciferase as a reporter.[9,10] This OR6 reporter assay system has enabled prompt and precise quantification of HCV

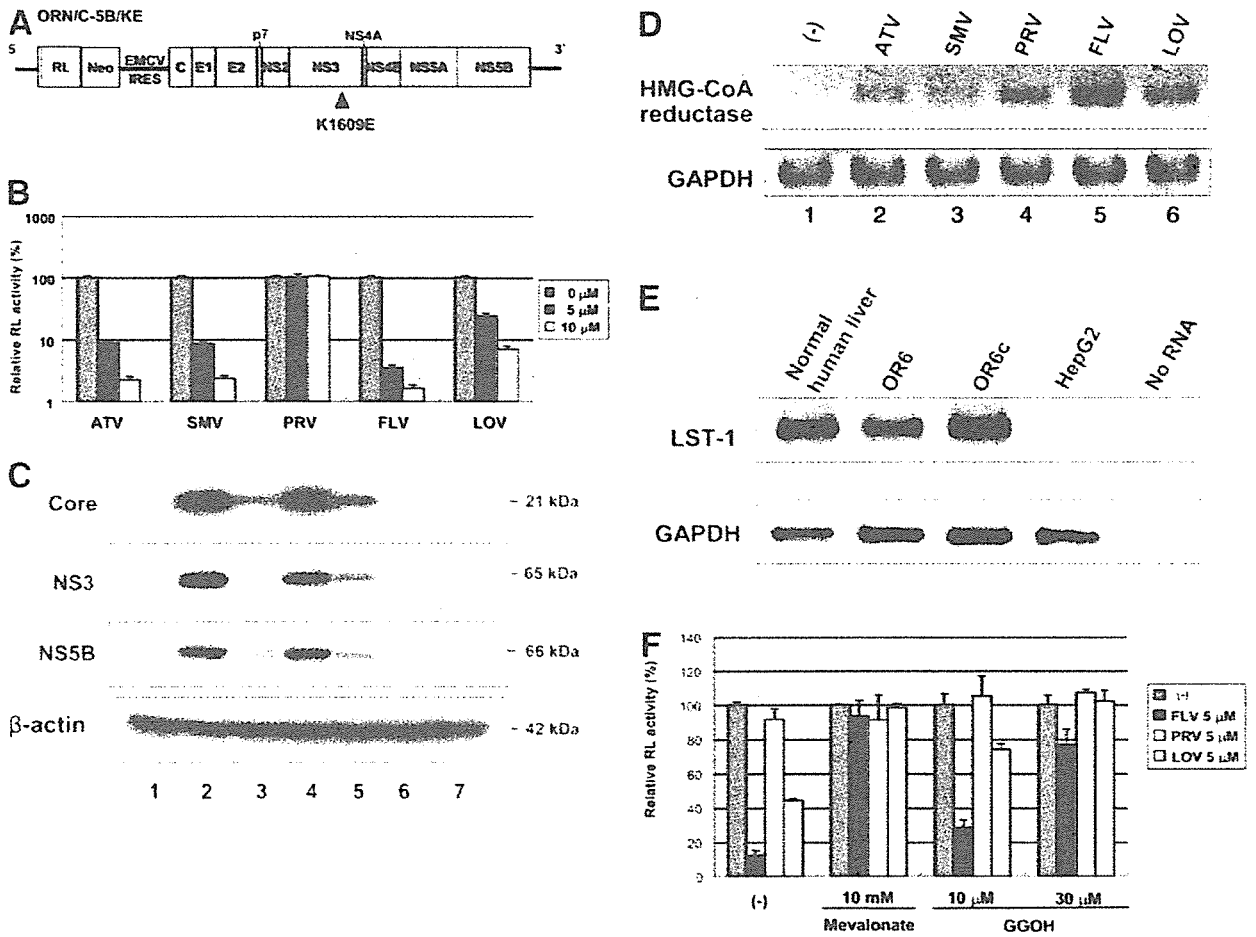

Fig. 1. Different inhibitory effects of various statins on HCV RNA replication in OR6 cells. (A) Schematic gene organization of genome-length HCV RNA encoding the *RL* gene, ORN/C-5B/KE, replicating in OR6 cells. RL is expressed as a fusion protein with Neo. The position of an adaptive mutation, K1609E, is indicated by a triangle. (B) Reporter assay on statin sensitivity of HCV RNA replication. OR6 cells were treated with ATV, SMV, PRV, FLV, and LOV (0, 5, and 10 μmol/L each). After 72 hours of treatment, the RL assay was performed as described in the Materials and Methods section. Shown here is the relative RL activity (%) calculated when the RL activity of untreated cells was assigned as 100%. The data indicate means ± SDs of triplicates from three independent experiments. (C) Western blot analysis of statin sensitivity of HCV RNA replication: lane 1, cured OR6 cells (OR6c) used as a negative control; lane 2, untreated OR6 cells; lane 3, OR6 cells treated with IFN-α (10 IU/mL); lane 4, OR6 cells treated with PRV (5 μmol/L); lane 5, OR6 cells treated with LOV (5 μmol/L); lane 6, OR6 cells treated with FLV (5 μmol/L); lane 7, OR6 cells treated with FLV (10 μmol/L). After 96 hours of treatment, the production of Core, NS3, and NS5B was analyzed by immunoblotting using anti-Core, anti-NS3, and anti-NS5B antibodies, respectively. β-actin was used as a control for the amount of protein loaded per lane. (D) Feedback induction of HMG-CoA reductase after treatment of statins: lane 1, untreated OR6c cells; lane 2, OR6c cells treated with ATV (10 μmol/L); lane 3, OR6c cells treated with SMV (10 μmol/L); lane 4, OR6c cells treated with PRV (10 μmol/L); lane 5, OR6c cells treated with FLV (10 μmol/L); lane 6, OR6c cells treated with LOV (10 μmol/L). After 24 hours of treatment, RT-PCR for HMG-CoA reductase was performed as described in the Materials and Methods section. RT-PCR for GAPDH was performed as an internal control. RT-PCR products (376 bp for HMG-CoA reductase and 334 bp for GAPDH) were detected by staining with ethidium bromide after 3% agarose gel electrophoresis. (E) RT-PCR analysis of LST-1 mRNA. Total RNA was extracted from OR6, OR6c, and HepG2 cells and subjected to RT-PCR analysis with primer sets for LST-1 (241 bp) and GAPDH (334 bp) as described in (D). Normal human liver total RNA (Clontech) was used as a positive control for LST-1. (F) Mevalonate and geranylgeraniol restore HCV RNA replication in statin-treated cells. OR6 cells were treated with FLV, PRV, and LOV (5 μmol/L each) alone or in the presence of mevalonate (10 mmol/L) or geranylgeraniol (GGOH, 10 and 30 μmol/L). After 72 hours of treatment, the RL assay was performed as described in (B).

RNA replication. Therefore, in the present study, we examined whether several types of statins currently used in clinical therapy exhibit anti-HCV activity, as has already been reported for LOV.[11,12] This time, the antiviral activities of five statins—ATV, FLV, LOV, PRV, and SMV—were tested using the OR6 assay system (Fig. 1A). The results revealed that ATV, FLV, and SMV exhibited stronger anti-HCV activity than did LOV and that FLV exhibited the strongest anti-HCV activity among the statins tested (Fig. 1B). Surprisingly, however, PRV had no inhibitory effect on HCV RNA replication (Fig. 1B). Similar results were obtained from the analysis of the ex-

pression levels of HCV proteins (Fig. 1C). The anti-HCV activity of 5 μmol/L FLV was compatible with that of 10 IU/mL IFN-α (Fig. 1C).

To exclude the possibility that only PRV was unable to inhibit HMG-CoA reductase, we examined the expression of HMG-CoA reductase in statin-treated OR6c cells by RT-PCR, because HMG-CoA reductase was known to show positive feedback when statins were active in the cells.[18] OR6c cells were treated with statins in the same way as were the OR6 cells used to measure the anti-HCV activity of statins, except that sampling for RT-PCR was performed after 24 hours of statin treatment. All statins, including PRV, enhanced expression of the HMG-CoA reductase gene (Fig. 1D). Although PRV is hydrophilic and does not cross cellular membranes passively, it has been reported that a human liver–specific organic anion transporter, LST-1, mediates the uptake of PRV in human hepatocytes but not in HepG2 cells, which showed very low PRV uptake.[19,20] Therefore, we examined the expression levels of LST-1 in OR6 and OR6c cells using an RT-PCR method. OR6 and OR6c cells expressed LST-1 at levels equivalent to that in normal human liver, confirming that LST-1 was not expressed in the HepG2 cells (Fig. 1E). These findings suggest that PRV is taken up actively in OR6 and OR6c cells. In summary, these results indicate all statins tested inhibit HMG-CoA reductase and suggest the anti-HCV action of statins is not a result of direct inhibition of HMG-CoA reductase.

Regarding the mechanism underlying the anti-HCV action of statins, it has thus far been reported that the inhibitory effect of LOV can be overcome by the addition of mevalonate (the product of the HMG-CoA reductase reaction) or geranylgeraniol (a donor of prenyl groups for protein geranylgeranyl transferase reaction).[11,12] These observations suggest that some geranylgeranylated proteins are required for HCV RNA replication and that LOV blocks HCV RNA replication by depleting endogenous geranylgeranyl pyrophosphate (the mevalonate-derived donor of protein geranylgeranylation). To evaluate this mechanism, we examined the effects of mevalonate and geranylgeraniol on the anti-HCV activities of the statins used in this study. OR6 cells were treated with 5 μmol/L FLV, PRV, or LOV alone or in the presence of mevalonate (10 mmol/L) or geranylgeraniol (10 or 30 μmol/L). Mevalonate and geranylgeraniol restored HCV RNA replication in the statin-treated cells, although 10 μmol/L geranylgeraniol exhibited partial restoration (Fig. 1F). In addition, we observed that the anti-HCV activities of the statins could be blocked by the addition of geranylgeranyl pyrophosphate (20 μmol/L) in the OR6 cells (data not shown), indicating geranylgeranyl pyrophosphate is also taken up in OR6 cells. These findings support two previous reports[11,12] that found the inhibition of HCV RNA replication by statins was not correlated with their cholesterol-lowering activities, although the reason for the lack of anti-HCV activity by PRV remains vague.

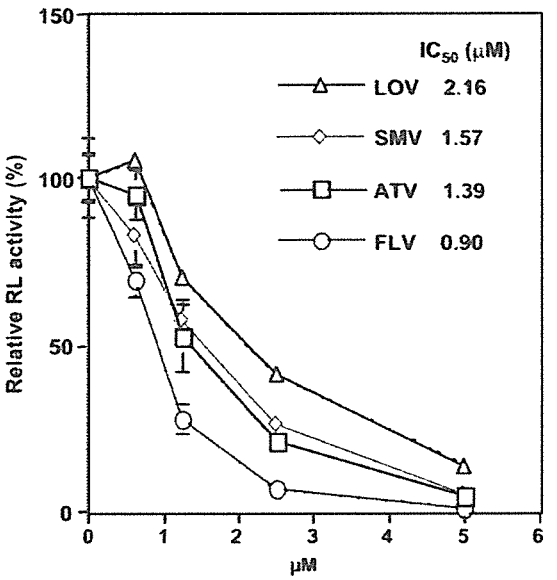

Fig. 2. Dose-dependent inhibition of HCV RNA replication by statins. OR6 cells were treated with LOV, SMV, ATV, and FLV at concentrations of 0.625, 1.25, 2.5, and 5 μmol/L. After 72 hours of treatment, the RL assay was performed, and RL activity was calculated as shown in Fig. 1B.

Anti-HCV Activity of FLV Significantly Stronger Than Those of Other Statins. From the dose-response curves after 72 hours of treatment with the statins, the concentrations of FLV, ATV, SMV, and LOV required for a 50% reduction in RL activity (IC_{50}) were calculated to be 0.90, 1.39, 1.57, and 2.16 μmol/L, respectively (Fig. 2). Consistent with the results shown in Fig. 1, the anti-HCV activity of FLV ($P < .01$ at 0.625-5 μmol/L), ATV ($P < .05$ at 1.25 μmol/L; $P < .01$ at 2.5 and 5 μmol/L), and SMV ($P < .05$ at 0.625 and 1.25 μmol/L; $P < .01$ at 2.5 and 5 μmol/L) was significantly stronger than that previously reported for LOV. In addition, the anti-HCV activity of FLV was significantly stronger than those of SMV ($P < .01$ at 1.25-5 μmol/L) and ATV ($P < .05$ at 1.25 μmol/L; $P < .01$ at 2.5 and 5 μmol/L).

Anti-HCV Activity of Statins Not Due to Their Cytotoxicity. Since it has been reported that the proliferation of the HCV replicon is dependent on host-cell growth,[21] it remained to be clarified whether the inhibitory effects of statins on HCV RNA replication were caused by their cytotoxicity. To examine this possibility, we investigated the cytotoxic effects of statins on OR6 cells. A comparison of cell viability in the untreated cells with that in the cells treated with each statin (5 μmol/L each) showed no significant decrease in the number of

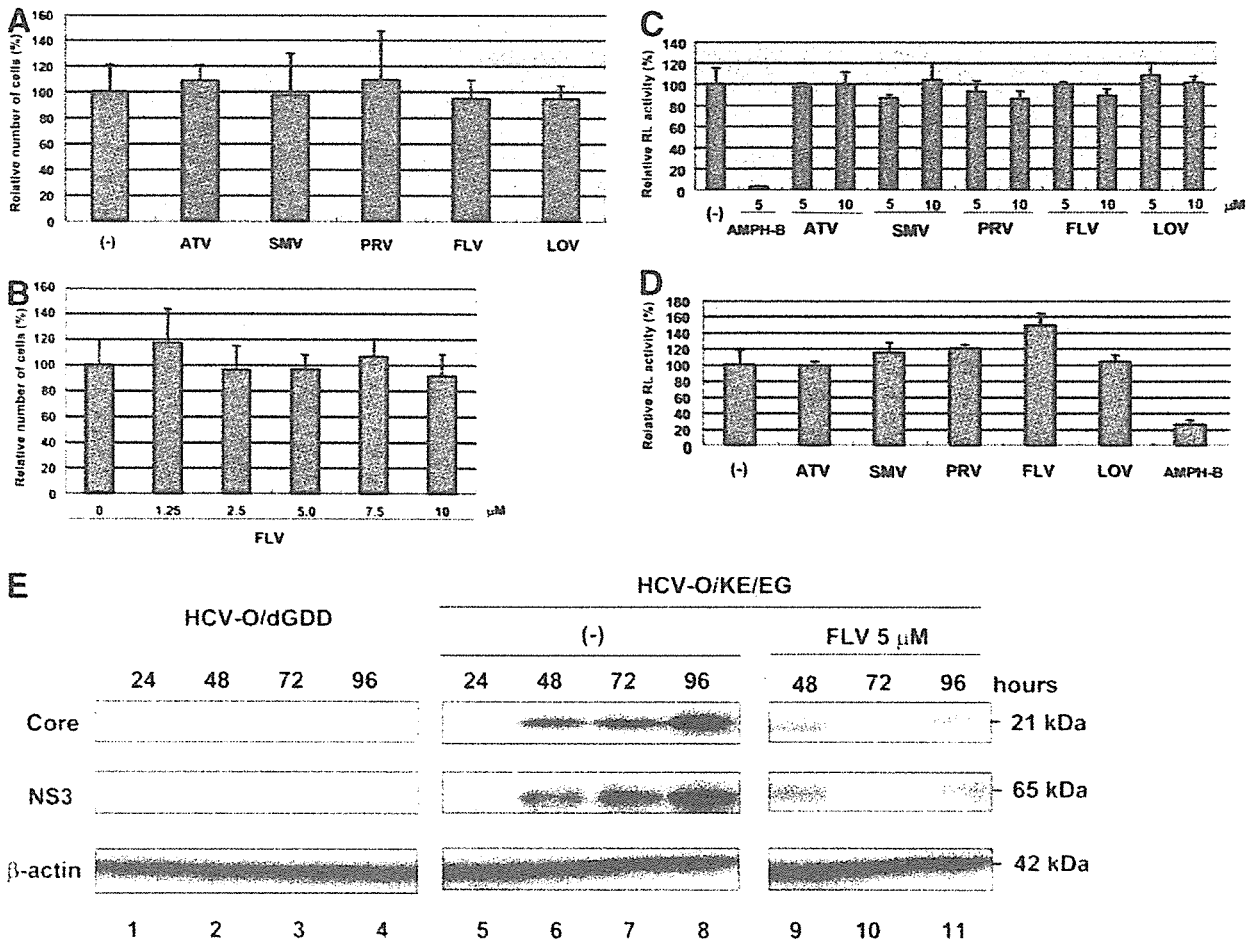

Fig. 3. Anti-HCV activity of the statins was not a result of inhibition of cell growth, RL activity, or EMCV IRES activity. (A) Cell viability after treatment with the statins. OR6 cells were cultured in the absence and in the presence of ATV, SMV, PRV, FLV, and LOV (5 μmol/L each), and then the number of viable cells was counted after trypan blue dye treatment. Shown here is the relative cell number (%) calculated when the cell number of untreated cells was assigned as 100%. The data indicate means ± SDs of triplicates from two independent experiments. (B) Cell viability after treatment with FLV. OR6 cells were cultured in the absence and in the presence of FLV (1.25, 2.5, 5, 7.5, and 10 μmol/L) for 72 hours, and then the number of viable cells was counted as described in (A). (C) No inhibition of RL activity by the statins. ATV, SMV, PRV, FLV, and LOV (5 or 10 μmol/L each) were directly added to the cell lysates from OR6 cells, and then the RL assay was performed. The relative RL activity was calculated as shown in Fig. 1B. AMPH-B (5 μmol/L) was used as a control reagent, which directly affected RL activity. (D) No inhibition of EMCV IRES activity by the statins. After pEMCV-RL was introduced into the OR6c cells, the cells were treated with ATV, SMV, PRV, FLV, and LOV (5 μmol/L each). After 72 hours of treatment, the RL assay was performed. Relative RL activity was calculated as shown in Fig. 1B. AMPH-B (2.5 μmol/L) was used as a control reagent, which directly affected RL activity. (E) Replication of authentic HCV RNA prevented by the statins. Authentic HCV-O RNA, HCV-O/KE/EG RNA, was introduced into the OR6c cells by electroporation as described previously.[3] After 24 (lane 5), 48 (lane 6), 72 (lane 7), and 96 (lane 8) hours of electroporation, production of Core and NS3 was analyzed by immunoblotting using anti-Core and anti-NS3 antibodies. Production of Core and NS3 after 24 (lane 1), 48 (lane 2), 72 (lane 3), and 96 (lane 4) hours of electroporation of HCV-O/dGDD RNA (negative control) was also analyzed. After 24 hours of electroporation of HCV-O/KE/EG RNA, the cells were treated with FLV (5 μmol/L), and then production of Core and NS3 was analyzed after 48 (lane 9), 72 (lane 10), and 96 (lane 11) hours of electroporation. β-actin was used as a control for the amount of protein loaded per lane.

cells following treatment with statins (Fig. 3A). However, it was recently reported that statins inhibited the proliferation of hepatocellular carcinoma cell lines (HuH-7 and HepG2) by inducing apoptosis and G1/S cell-cycle arrest.[22] Because that study found the IC_{50} of FLV in HuH-7 cells to be 10 ± 3 μmol/L, we further examined the effects of FLV on the proliferation of OR6 cells by varying the concentration (up to 10 μmol/L) of FLV. FLV (at least at concentrations ≤ 10 μmol/L) did not inhibit the proliferation of OR6 cells (Fig. 3B), suggesting that FLV does not induce apoptosis or G1/S cell-cycle arrest in OR6 cells, although the OR6 cell line is a HuH-7-derived cell line.[10] In summary, these results indicate that none of the statins showed any cytotoxicity to the OR6 cells at the concentrations used in our assay system. This suggests the statins possess the

ability to inhibit replication of HCV RNA via specific antiviral mechanism(s).

Anti-HCV Activity of Statins Not Due to Inhibition of RL Activity. We clearly showed that the anti-HCV activities of statins were not due to their cytotoxicity. However, it remained to be clarified whether the statins used in this study would directly inhibit RL activity, because we recently found that two antifungal compounds, amphotericin B (AMPH-B) and nystatin, drastically inhibited RL activity (Ikeda et al., unpublished data). To examine this possibility, we investigated the effects of statins on RL activity. The addition of the statins to cell lysates prepared from OR6 cells revealed that none of the statins (up to 10 μmol/L) tested exhibited any inhibitory effect on RL activity, although AMPH-B extensively inhibited RL activity (Fig. 3C). This result excludes the possibility that the statins directly inhibit RL activity.

Anti-HCV Activity of Statins Not Due to Inhibition of EMCV IRES Activity. To further exclude the possibility that the anti-HCV activities of statins were a result of the artificial assay system, we next tested the possibility that the statins inhibit EMCV IRES activity, because Core-NS5B is translated in an EMCV-IRES-dependent manner in OR6 cells. The plasmid encoding RL driven by EMCV IRES was transfected into the OR6c cells, and 24 hours after transfection the cells were treated with each statin (5 μmol/L each) for 72 hours. The results revealed none of the statins exhibited any inhibitory effect, although AMPH-B drastically inhibited RL activity again (Fig. 3D). These data suggest the statins had no effect on exogenous genes EMCV IRES and RL introduced into HCV RNA.

Statins Prevent Replication of Authentic HCV RNA. To obtain further evidence that the statins prevent HCV RNA replication, we prepared authentic HCV-O-derived genome-length HCV RNA possessing two adaptive mutations (HCV-O/KE/EG). One adaptive mutation, K1609E in NS3, was previously described,[9] and the other, E1202G in NS3, was found in OA cells harboring genome-length HCV-O RNA (Abe et al., in preparation). The combination of these two mutations markedly enhanced the efficiency of HCV RNA replication, and HCV proteins were continuously detected for at least 8 weeks (Abe et al., in preparation). HCV-O/dGDD, from which the GDD motif in NS5B polymerase was deleted, was used as a control. HCV-O/KE/EG and HCV-O/dGDD RNAs were transfected into OR6c cells, and the production of HCV proteins was monitored for 96 hours. The Core and NS3 in the OR6c cells transfected with HCV-O/dGDD RNA were not detected even 96 hours after transfection. However, the Core and NS3 in the OR6c cells transfected with HCV-O/KE/EG RNA were detected 24 hours after transfection, and their expression increased with time (Fig. 3E). This observation suggests that HCV-O/KE/EG RNA, without exogenous genetic factors such as EMCV IRES and RL, efficiently replicates in OR6c cells. Using such a transient HCV RNA replication system, we demonstrated that the production of Core and NS3 was markedly prevented when the OR6c cells transfected with HCV-O/KE/EG RNA were treated with FLV (5 μmol/L) at 24 hours after transfection (Fig. 3E). In summary, our results indicate that the statins prevent HCV RNA replication and that their inhibitory effects are not a result of the inhibitory effect toward the exogenous genes introduced into ORN/C-5B RNA replicating in OR6 cells.

Combination of a Statin with IFN Efficiently Enhances Anti-HCV Activity of IFN. IFN is the world standard of therapy for CH C, and currently its best partner is ribavirin. Because we found the statins efficiently inhibited HCV activity, we expected the statins to be candidates for use in combination with IFN. To address this point, we examined the inhibitory effects of combinations of IFN-α (0, 2, 4, and 8 IU/mL) and the statins (5 μmol/L each) using the OR6 assay system. As expected, ATV, SMV, FLV, and LOV markedly enhanced the anti-HCV effect of IFN-α, although PRV did not (Fig. 4A). In combination with IFN-α, FLV again was the statin that had the strongest effect. The results indicated that cotreatment was more effective than treatment with IFN-α alone. We thought the mechanism underlying this phenomenon might be statin-induced enhancement of the type I IFN signaling pathway. To examine this possibility, we investigated the phosphorylation status of STAT1 after statin treatment. The results revealed that FLV did not cause phosphorylation of STAT1 in OR6c or OR6 cells, although IFN-α did so efficiently in both types of cells (Fig. 4B). In addition, we confirmed that phosphorylation of STAT2 and STAT3 in both cell types was also not induced by FLV treatment (data not shown). Furthermore, we confirmed that FLV did not affect expression of 2′-5′-OAS1 mRNA and that the expression level induced by IFN-α treatment was not affected by treatment with FLV (Fig. 4C). PRV, which showed no anti-HCV activity, also had no effect on the type I IFN signaling pathway. In summary, these results indicate the statin-induced enhancement of the anti-HCV action of IFN-α is not a result of induction of the type I IFN signaling pathway.

Cotreatment of IFN-α and FLV Exhibits Synergistic Inhibitory Effects on HCV RNA Replication. We showed that FLV was the statin tested that exhibited the strongest anti-HCV activity, not only alone, but also in combination with IFN-α. Therefore, we focused on the anti-HCV activity of FLV, minutely examining the in-

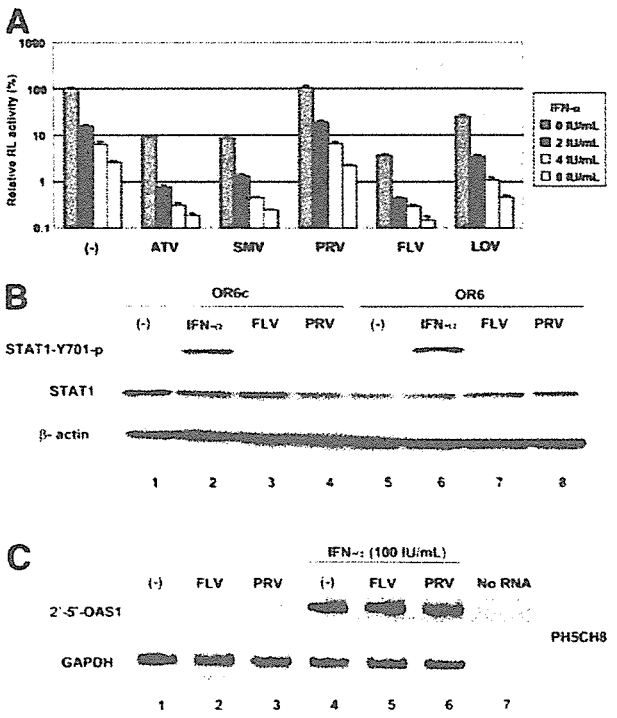

Fig. 4. Statins enhance inhibition of HCV RNA replication because of IFN-α. (A) Effects of statins on the anti-HCV activity of IFN. OR6 cells were cotreated with IFN-α (0, 2, 4, and 8 IU/mL) and ATV, SMV, PRV, FLV, or LOV (5 μmol/L each). The RL assay was performed, and the relative RL activity was calculated as shown in Fig. 1B. (B) No enhancement of type I IFN signaling by the statins. OR6c or OR6 cells were cultured for 2 hours in the absence and in the presence of IFN-α (100 IU/mL), FLV (10 μmol/L), and PRV (10 μmol/L), and the cells were subjected to Western blot analysis of STAT1 and its phosphorylation status. β-actin was used as a control for the amount of protein loaded per lane. (C) No induction of the IFN-inducible gene by the statins. PH5CH8 cells were untreated or were treated with FLV (10 μmol/L) and PRV (10 μmol/L) for 2 hours, and then total RNA extracted from the cells was subjected to RT-PCR for 2′-5′-OAS1 (25 cycles). The PH5CH8 cells were treated for 9 hours with IFN-α (100 IU/mL) alone or in combination with FLV (10 μmol/L) or PRV (10 μmol/L), and then RT-PCR for 2′-5′-OAS1 was performed. The RT-PCR products (358 bp for 2′-5′-OAS1 and 334 bp for GAPDH) were detected, as shown in Fig. 1D.

hibitory effects of the combination of IFN-α and FLV on genome-length HCV RNA replication. A dose-response curve of FLV was obtained for fixed concentrations of IFN-α of 0, 4, 8, 16, 32, and 64 IU/mL. The results revealed the curves shifted to shift markedly to the bottom as the concentration of IFN-α increased (Fig. 5A), indicating that cotreatment was drastically more effective than treatment with IFN-α alone. Furthermore, we observed that RL activity decreased to almost the background level in the OR6 reporter assay when OR6 cells were cotreated with 64 IU/mL of IFN-α and FLV at concentrations above 1.25 μmol/L (Fig. 5A). Because the data in Fig. 5A indicate the possibility of a synergistic effect of the combination of IFN-α and FLV, we examined whether the effect of this combination is synergistic or additive effect using an isobologram method.[23,24] The anti-HCV activities of IFN-α and FLV in combination were evaluated by the OR6 reporter assay. Dose-response inhibition of HCV RNA replication was evaluated for varying IFN-α concentrations (0-8 IU/mL) in the presence of various doses of FLV (0-7.5 μmol/L). The IC_{90} values of IFN-α and FLV were 4.0 IU/mL and 6.7 μmol/L, respectively. These data were used to generate isoboles, which demonstrated 90% inhibition of HCV RNA replication, and the synergistic anti-HCV action of IFN-α and FLV was revealed by the curvilinear plots of the 90% isoboles (Fig. 5B). In conclusion, we clearly demonstrated that combination treatment of IFN-α and FLV was an overwhelmingly more effective treatment,

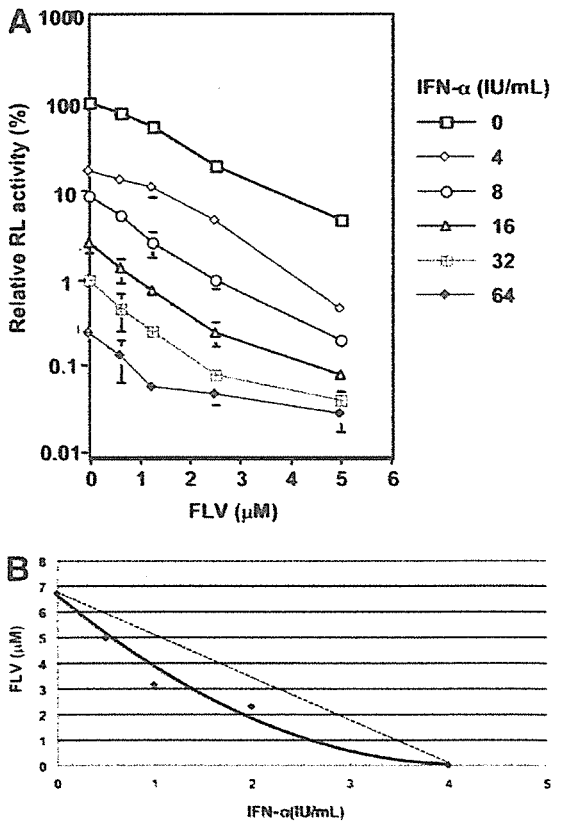

Fig. 5. Synergistic effect of FLV in combination with IFN-α on HCV RNA replication. (A) Effect of FLV in combination with IFN-α. OR6 cells were cotreated with FLV (0, 0.625, 1.25, 2.5, and 5 μmol/L) and IFN-α (0, 4, 8, 16, 32, and 64 IU/mL). The RL assay was performed after 72 hours of treatment, and the relative RL activity was calculated as shown in Fig. 1B. (B) Isobole plots of 90% inhibition of HCV RNA replication. OR6 cells were treated with IFN-α (0, 0.5, 1, 2, 4, 6, and 8 IU/mL) in combination with FLV (0, 0.625, 1.25, 2.5, 5, and 7.5 μmol/L) for 72 hours, and the RL assay was performed as shown in Fig. 1B to obtain 90% isoboles. The broken line indicates the additive effect in the isobologram method used.[23,24]